Türkiye Jeoloji Bülteni
Geological Bulletin of Turkey
65 (2022) 93—116
doi:10.25288/tjb.1015537

The Anatolian Diagonal: A Broad Left-Lateral Shear Zone Between the North Anatolian Fault Zone and the Aegean / Cyprus Arcs

Anadolu Çaprazı: Kuzey Anadolu Fay Zonu ile Ege / Kıbrıs Yayları Arasında Geniş Bir Sol Yanal Makaslama Zonu

**Gürol Seyitoğlu[1*], Esra Tunçel[2], Bülent Kaypak[3]
Korhan Esat[1], Ergin Gökkaya[2]**

[1] Department of Geological Engineering, Tectonics Research Group, Ankara University, 06830 Ankara, Türkiye.
[2] Department of Geography, Ankara University, 06100 Ankara, Türkiye.
[3] Department of Geophysical Engineering, Ankara University, 06830 Ankara, Türkiye.

• Geliş/Received: 27.10.2021 • Düzeltilmiş Metin Geliş/Revised Manuscript Received: 10.01.2022 • Kabul/Accepted: 13.01.2022
• Çevrimiçi Yayın/Available online: 02.02.2022 • Baskı/Printed: 15.04.2022
Araştırma Makalesi/Research Article *Türkiye Jeol. Bül. / Geol. Bull. Turkey*

Abstract: Recent detailed examination of the internal deformation of the Turkish-Iranian Plateau in the hinterland of Bitlis-Zagros Suture Zone, which is related to the collision of the Arabian and Eurasian plates, indicates multiple intersection points between the right- and left-lateral strike-slip structures explained by an inevitably broad left-lateral strike-slip shear zone, the Anatolian Diagonal.

The faults bounding and internally deforming the Anatolian Diagonal were closely examined by using high-resolution satellite images, focal mechanism solutions of the earthquakes, and published seismic reflection data in the offshore areas. The Anatolian Diagonal is a NE-SW trending left-lateral shear zone having a 170 km width between the Central Anatolian and the East Anatolian fault zones and an 850 km length between Erzincan and the Cyprus Arc. It has at least four intersection points with the right-lateral North Anatolian Fault Zone and the Southeast Anatolian-Zagros Fault Zone. As the offshore continuation of the Ecemiş-Deliler Fault of the Anatolian Diagonal, the Biruni Fault reaches the Cyprus Arc and Piri Reis (Mediterranean) Ridge Front west of Cyprus. This structure creates a restraining stepover with the left-lateral Antalya-Kekova Fault Zone and causes NW-SE trending thrusts of the Florence Rise and Antalya Thrust in the Antalya Basin. There is another restraining stepover between the Antalya-Kekova Fault Zone and the Pliny-Strabo Fault Zone, where the thrust-controlled northern margin of Rhodes basin developed.

In this neotectonic framework, there is no need for the existence of the highly-debated left-lateral Fethiye-Burdur Fault Zone as an onshore continuation of the Pliny and Strabo faults. In fact, the westerly motion of the Anatolian plate is accommodated by the left-lateral Anatolian Diagonal Shear Zone, Antalya-Kekova Fault Zone and Pliny-Strabo Fault Zone together with the right-lateral North Anatolian Fault Zone.

Keywords: Anatolian Diagonal, Cyprus, East Anatolian Fault Zone, Eastern Mediterranean, Neotectonics.

Öz: *Türk-İran Platosu, Arap ve Avrasya levhalarının çarpışmaları ile ilişkili Bitlis-Zagros Kenet Zonu'nun ard ülkesinde yer alır. Platonun iç deformasyonunun yakın zamanda ayrıntılı biçimde incelenmesi, sağ ve sol yanal doğrultu atımlı yapıların çoklu kesişme noktalarının varlığını ortaya çıkarmış ve bu kaçınılmaz olarak Anadolu Çaprazı adı ile anılan geniş sol yanal makaslama zonu ile açıklanmıştır.*

Correspondence / *Yazışma*: seyitoglu@ankara.edu.tr

http://tjb.jmo.org.tr
http://dergipark.gov.tr/tjb

Anadolu Çaprazı'nı sınırlayan ve iç deformasyonuna neden olan faylar, yüksek çözünürlüklü uydu görüntüleri, depremlerin odak mekanizması çözümleri ve deniz alanlarındaki yayınlanmış sismik yansıma kesitleri yardımıyla incelenmiştir. Anadolu Çaprazı, Orta Anadolu Fay Zonu ile Doğu Anadolu Fay Zonu arasında 170 km genişliğe ve Erzincan ile Kıbrıs Yayı arasında 850 km uzunluğa sahip, KD-GB yönelimli bir sol yanal makaslama zonudur. Bu zon, Kuzey Anadolu Fay Zonu ve Güneydoğu Anadolu-Zagros Fay Zonu ile en az dört kesişim noktasına sahiptir. Anadolu Çaprazı'na ait Ecemiş-Deliler Fayı'nın Akdeniz'deki uzanımı olan Biruni Fayı, Kıbrıs Yayı'na ve Piri Reis Sırtı'na (Mediterranean Ridge) Kıbrıs'ın batısında ulaşmaktadır. Bu yapı, Antalya – Kekova Fay Zonu ile daralmalı sıçrama oluşturmakta olup, bu nedenle Antalya havzasında KB-GD doğrultulu bindirmeler ile temsil edilen Florence Yükselimi ve Antalya Bindirmesi meydana gelmiştir. Diğer bir daralmalı sıçrama alanı ise Antalya-Kekova Fay Zonu ile Pliny-Strabo Fay Zonu arasında gelişmiş olup, burada Rodos havzasının bindirmeler ile kontrol edilen kuzey kenarı bulunmaktadır.

Bu neotektonik çerçeve içinde, varlığı oldukça tartışmalı olan Pliny ve Strabo faylarının karadaki devamı olarak değerlendirilen sol yanal Fethiye – Burdur Fay Zonu'na ihtiyaç bulunmamaktadır. Aslında, Anadolu Levhasının batıya hareketi, sol yanal Anadolu Çaprazı Makaslama Zonu, Antalya-Kekova Fay Zonu ve Pliny-Strabo Fay Zonu ile sağ yanal Kuzey Anadolu Fay Zonu tarafından karşılanmaktadır.

Anahtar Kelimeler: *Anadolu Çaprazı, Doğu Akdeniz, Doğu Anadolu Fay Zonu, Kıbrıs, Neotektonik.*

INTRODUCTION

In the neotectonic framework of the Eastern Mediterranean, the definition of plate boundaries has not changed significantly from the beginning of plate tectonics theory to GPS-based studies (McKenzie, 1970; 1972; Reilinger et al., 1997). However, GPS-derived velocity field data has initiated discussion about whether the slab pull in the Aegean Arc or the westward push due to the collision of Arabian and Eurasian plates is the driving mechanism of westward movement of the Anatolian plate (Reilinger et al., 1997; 2006; Chorowicz et al., 1999; McClusky et al., 2000; Şengör et al., 2004; Le Pichon and Kreemer, 2010).

In the neotectonic period, the Anatolian plate moved westward along the left-lateral East Anatolian Fault Zone (EAFZ) and right-lateral North Anatolian Fault Zone (NAFZ) (McKenzie, 1972; Şengör, 1980; Şengör et al., 1985) after the collision of the Arabian and Eurasian plates. This classical view offers a triple junction at Karlıova (Figure 1). Recently, Şengör et al. (2019) proposed an "asymmetric Karlıova triple junction model", keeping the earlier single intersection vision to explain higher slip rates on the NAFZ relative to the EAFZ.

On the other hand, a recent paper concerning the internal deformation of the Turkish-Iranian Plateau in the hinterland of Bitlis-Zagros Suture Zone (BZSZ) introduces a rhomboidal cell model to explain the relationship between left- and right-lateral faults in the region (Seyitoğlu et al., 2018). Some margins of these cells align in a certain direction and constitute region-wide shear zones. For example, the southwest strike-slip margins of the Çayırlı, Beşgöze and Hınıs rhomboidal cells indicate that the NAFZ continues beyond Karlıova towards the east until Lake Van and creates a releasing stepover with the Southeast Anatolian-Zagros Fault Zone (SAZFZ), including the Main Recent Fault of Zagros Mountains in Iran. In this concept, the SAZFZ is terminated by the left-lateral Ovacık Fault (OVF) in the northwest and offsets the EAFZ in Bingöl (Seyitoğlu et al., 2018) (Figure 1). This approach offers multiple intersection points between the right- and left-lateral strike-slip structures contrary to the classical tectonic escape model (Şengör et al., 1985) and inevitably requires a broad left-lateral shear zone, which is named here as the Anatolian Diagonal Shear Zone.

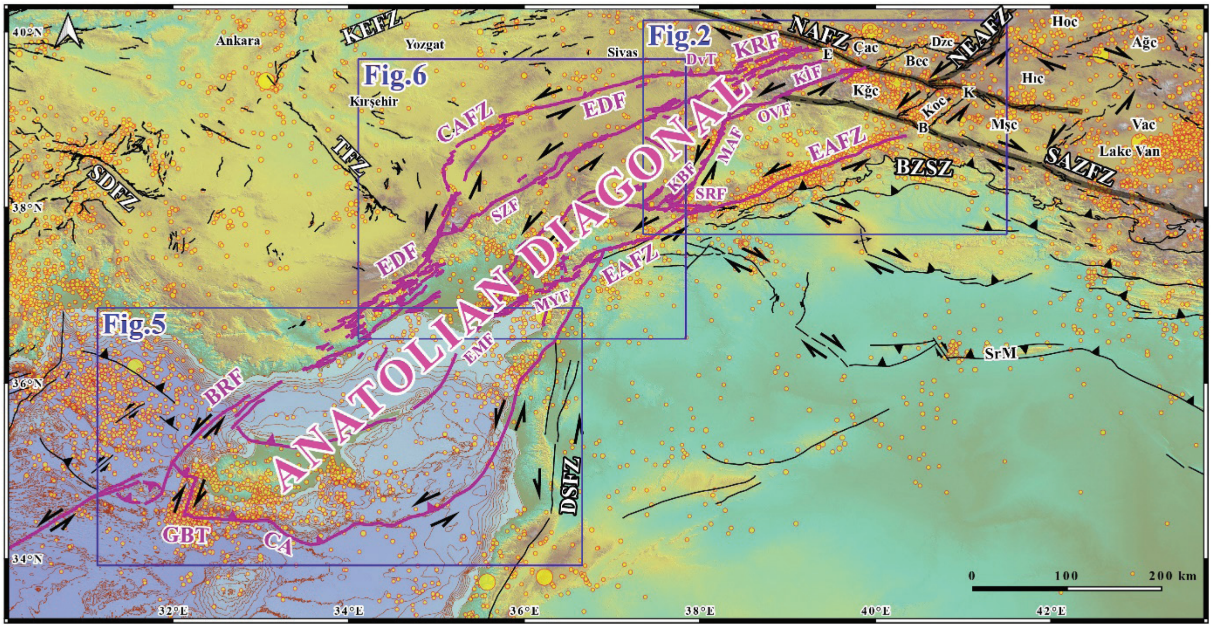

Figure 1. Neotectonic Anatolian Diagonal. It is a left-lateral shear zone limited by the CAFZ and EAFZ and extending from the NAFZ to the Cyprus Arc. Fault lines are from Emre et al. (2013), Seyitoğlu et al. (2017, 2018) and this paper. The epicenter locations are from the ISC Catalogue (M≥3.5). For the focal mechanism solutions, see Appendix B. E: Erzincan; K: Karlıova; B: Bingöl; NAFZ: North Anatolian Fault Zone; NEAFZ: Northeast Anatolian Fault Zone; SAZFZ: Southeast Anatolian-Zagros Fault Zone; BZSZ: Bitlis-Zagros Suture Zone; SrM: Sincar Mountains; EAFZ: East Anatolian Fault Zone; DSFZ: Dead Sea Fault Zone; CAFZ: Central Anatolian Fault Zone; KEFZ: Kırıkkale-Erbaa Fault Zone; TGFZ: Tuz Gölü Fault Zone; SDFZ: Sultandağları Fault Zone; KRF: Karaca Fault; KİF: Kemah-İliç Fault; OVF: Ovacık Fault; MAF: Malatya Fault; SZF: Sarız Fault; EDF: Ecemiş-Deliler Fault; BRF: Biruni Fault; GBT: Gazibaf Transform; CA: Cyprus Arc; EMF: Elbistan-Misis Fault; MYF: Maraş-Yumurtalık Fault; KBF: Kantarma-Barış Fault; SRF: Sürgü Fault; DvT: Divriği Thrust. The rhomboidal cells are of Seyitoğlu et al. (2018): Çac: Çayırlı cell; Dzc: Düzyurt cell; Bec: Beşgöze cell; Hoc: Horasan cell; Hıc: Hınıs cell; Ağc: Ağrı cell; Vac: Van cell; Mşc: Muş cell; Koc: Karlıova cell; Kğc: Kiğı cell.

Şekil 1. *Anadolu Çaprazı'nın neotektonik anlamı. Orta Anadolu Fay Zonu ve Doğu Anadolu Fay Zonu tarafından sınırlanan, Kuzey Anadolu Fay Zonu ile Kıbrıs Yayı arasında uzanan sol yanal makaslama zonu. Fay hatları Emre vd. (2013), Seyitoğlu vd. (2017; 2018) ve bu makaleden alınmıştır. Deprem dış merkez dağılımı ISC kataloğundan (M≥3.5) alınmıştır. Odak mekanizması çözümleri için Appendix B'ye bakınız.*

The term "Anatolian Diagonal" was defined by Davis (1971) to explain the biological diversity between east and central Anatolia. Its geomorphological meaning has recently been discussed by Kuzucuoğlu et al. (2019). The neotectonic mean of the Anatolian Diagonal simply corresponds to a left-lateral shear zone limited by the East Anatolian Fault Zone (EAFZ) and Central Anatolian Fault Zone (CAFZ) between Erzincan and the Cyprus Arc (Figure 1).

In this paper, we aim to demonstrate the details of the multiple intersection points between the left- and right-lateral structures creating the broad left-lateral strike-slip shear zone, the Anatolian Diagonal. Another issue that needs to be clarified is the genetic relationship of the Anatolian Diagonal with the Aegean and Cyprus arcs, which forms an important part of the new neotectonic framework of Türkiye.

METHODS

The study area (Figure 1) covers more than 180,000 km^2 and contains several fault zones. Therefore, it is unavoidable to use high-resolution satellite imagery of Google Earth software to examine the morphotectonic features (Huang et al., 1993; Keller and Pinter, 2001; Zhang et al., 2004; Şengör, 2017; Reitman et al., 2019) and determine the active fault lines with the help of active fault maps (Emre et al., 2013) and geological maps / reports of the General Directorate of Mineral Research and Exploration (MTA) and other published papers (i.e., Kaymakçı et al., 2010; Yazıcı et al., 2018; Sançar et al., 2020). The detailed fault segments were mapped in the GIS environment and in limited parts of the study area, structural data were obtained from the faults. The offshore continuation of active faults was traced by using published seismic reflection sections. The elevation data for the land topography and bathymetry were obtained from the 1:25000 scale topographical maps and World Ocean Base by Esri (2021). To demonstrate the activity of fault segments apart from the morphological indicators, we provide epicenter locations and focal mechanism solutions of the seismic events where possible (Electronic Appendix A).

Focal mechanism solutions were either collected from various sources presented in Table 1 or directly computed using waveform data for significant earthquakes (Electronic Appendix B). The Regional Moment Tensor (RMT) inversion method (Herrmann, 2013) was performed for the focal mechanism solutions of earthquakes of magnitude 3.0 and greater. Three-component broadband waveform data for the RMT solutions were retrieved from Incorporated Research Institutions for Seismology Data Services (IRIS database, https://www.iris.edu, last accessed in January 2020) and the European Integrated Data Archive Service (http://www.orfeus-eu.org/data/eida). The furthermost epicentral distance was determined to be 700 km because of the inadequate number of nearby stations. Whole waveform data was recorded by the stations belonging to both national networks such as the Kandilli Observatory and Earthquake Research Institute (KOERI) as well as the Directorate of Disaster Affairs (AFAD) and the earthquake observation centers of neighboring countries. Almost all stations are equipped with velocity broadband seismometers. Because the same event locations were used as in the data provider agency, we did not perform any relocation procedure. Both the observed and synthetic Green's function ground velocities were cut from a range of 5–10 s before the P-wave's first-arrival to a range of 110–180 s after it. In the inversion process, a three-pole causal Butterworth bandpass filter with a 0.02–0.10 Hz band range was used for the events. However, 0.06-0.08 Hz bandpass filter range was preferred for most of the events. Additionally, an optional microseism rejection filter was applied to enhance the signal-to-noise ratio when needed. During the moment tensor inversion process, we eliminated noisy and problematic signals.

In order to follow the fault lines in detail, readers should consult the e-supplement data visible on Google Earth software (Electronic Appendix C).

NEOTECTONIC MEANING OF THE ANATOLIAN DIAGONAL

The Anatolian Diagonal is a 170 km wide NE-SW trending left-lateral strike-slip shear zone limited by the EAFZ and CAFZ. It has a length of 850 km between Erzincan and the Cyprus Arc (Figure 1).

The southeast margin of the Anatolian Diagonal is composed of the EAFZ (Herece, 2008; Duman and Emre, 2013; Emre et al., 2013, 2018). The northwest margin of the Anatolian Diagonal is represented by the CAFZ, which was defined by Koçyiğit and Beyhan (1998). On the other hand, its relationship with the Cyprus Arc at the southwest end and the NAFZ at the northeast end are poorly defined (Koçyiğit and Beyhan, 1998; Emre et al., 2013).

Table 1. Sources for the focal mechanism solutions used in this study.
Çizelge 1. Bu çalışmada odak mekanizma çözümleri için kullanılan kaynaklar.

Seismological Data Centers		
National	**Other Nations**	**International**
1) DDA: Republic of Turkey Prime Ministry Disaster and Emergency Management Authority, Earthquake Department (https://deprem.afad.gov.tr)	**1) ATH:** National Observatory of Athens (http://www.noa.gr)	**1) GCMT:** The Global Centroid Moment Tensor Catalog (Dziewonski et al., 1981; Ekström et al., 2012) (https://www.globalcmt.org)
2) KOERI: Boğaziçi University Kandilli Observatory and Earthquake Research Institute Regional Earthquake-Tsunami Monitoring Center (http://www.koeri.boun.edu.tr)	**2) USGS:** U.S. Geological Survey (https://www.usgs.gov)	**2) ISC:** International Seismological Centre (Lentas, 2018; Lentas et al., 2019) (http://www.isc.ac.uk)
3) ATA: Atatürk University Earthquake Research Center	**3) ZUR_RMT:** The Swiss Seismological Service (http://seismo.ethz.ch)	**3) MED-RCMT:** European-Mediterranean Regional Centroid-Moment Tensors (Pondrelli, 2002) (http://rcmt2.bo.ingv.it)
	4) GFZ: GFZ German Research Centre for Geosciences (https://geofon.gfz-potsdam.de/)	
Publications (papers, reports, thesis, etc.)		
Acarel et al. (2019); Ergin (1999); Ergin et al. (2004); Kılıç and Utkucu (2012); Kılıç et al. (2017); Ökeler (2003); Seyitoğlu et al. (2018)		

The internal deformation of the Anatolian Diagonal is taken by mainly left-lateral faults and minor right-lateral faults (Figure 1). The Anatolian Diagonal can be evaluated as a highly seismic zone, but some sections show low seismicity in the instrumental period (Figure 1).

Southeast Margin of the Anatolian Diagonal: The EAFZ

The East Anatolian Fault Zone (EAFZ) was defined by Arpat and Şaroğlu (1972) and Seymen and Aydın (1972) during examination of the surface ruptures of the 1971.04.22 Bingöl earthquake (Mb=5.9) between Karlıova and Bingöl (Figure 2). NW-SE trending surface ruptures were reported along with NE-SW trending left-lateral fault traces in Bingöl. Moreover, the unexpected seismic event of #75_2003.05.01 Bingöl earthquake (Mw=6.4) according to earthquake triggering models (Nalbant et al., 2002, 2005) and its source of NW-SE trending right-lateral strike-slip faults (Dirik et al., 2003) are allowed to interpret that the right-lateral SAZFZ cuts Göynük-Karlıova Fault (GKF) and emphasized that the EAFZ starts at Bingöl at the intersection point with the SAZFZ (Seyitoğlu et al., 2018, 2020) (Figure 2).

The EAFZ has been examined in detail by several researchers (Şaroğlu et al., 1992; Herece, 2008), but the segmentation of Duman and Emre (2013) has been followed in this paper. They defined several segments and declared that the Pütürge segment was a seismic gap, with an 11 km left-lateral displacement of the Fırat River. Recently, the 2020.01.24 Doğanyol-Sivrice earthquake (Mw=6.7) occurred in this segment (Melgar et al., 2020) (Figure 2). However, there is no agreement about the meeting point and the style of merging between the EAFZ and the Dead Sea Fault Zone (DSFZ) (see Rojay et al., 2001; Akyüz et al., 2006a; Duman and Emre, 2013) (Figure 1).

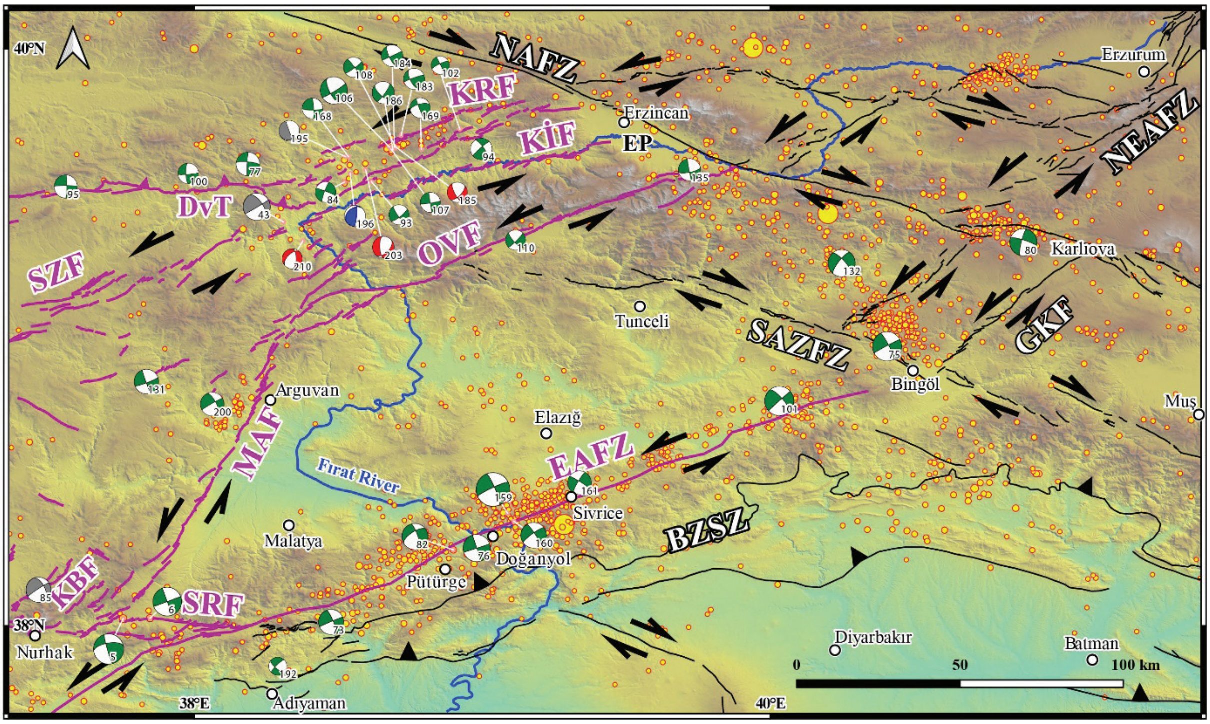

Figure 2. Northeast end of left-lateral Anatolian Diagonal and its relationship with the right-lateral structures. The fault lines are from Emre et al. (2013), Seyitoğlu et al. (2017, 2018) and this paper. Epicenter locations are from the ISC Catalogue (M≥3.5). See Appendix A and C for details of faults and Appendix B for the focal mechanism solutions. NAFZ: North Anatolian Fault Zone; EP: Erzincan Plain; NEAFZ: Northeast Anatolian Fault Zone; GKF: Göynük-Karlıova Fault; SAZFZ: Southeast Anatolian-Zagros Fault Zone; BZSZ: Bitlis-Zagros Suture Zone; EAFZ: East Anatolian Fault Zone; SRF: Sürgü Fault; KBF: Kantarma-Barış Fault; MAF: Malatya Fault; OVF: Ovacık Fault; KİF: Kemah-İliç Fault; KRF: Karaca Fault; DvT: Divriği Thrust; SZF: Sarız Fault.

Şekil 2. *Sol yanal Anadolu Çaprazı'nın kuzeydoğu ucu ve sağ yanal yapılarla ilişkisi. Fay hatları Emre vd. (2013); Seyitoğlu vd. (2017; 2018) ve bu makaleden alınmıştır. Dış merkez konumları ISC kataloğundan (M≥3.5) alınmıştır. Fayların detayları için Appendix A ve C'ye, odak mekanizmaları için Appendix B'ye bakınız.*

Northwest Margin of the Anatolian Diagonal: Its Relationship with the NAFZ

The details of the segment distribution between CAFZ and NAFZ were not presented by Koçyiğit and Beyhan (1998) but recently, Şengör et al. (2019) tried to explain this relationship with fish-bone faults. Although the fish-bone model was originally designed to explain the right-lateral faults veering from the NAFZ (i.e., Kırıkkale-Erbaa and Almus faults, see Şengör and Barka, 1992), the left-lateral Ovacık and Deliler faults were considered as fish-bone faults defining the Cappadocian Slice. There is an inconsistency between the fish-bone model and reality in the field, in fact, because the veering Ovacık and Deliler faults have the opposite sense of being shear zones (Şengör et al., 2019).

We propose that the structural connection between the CAFZ and NAFZ is provided by the newly determined Karaca Fault (KRF) and Kemah-İliç Fault (KİF) (Figure 2). The KRF and KİF are semi-parallel left-lateral faults, as indicated by the morphological data and focal mechanism of seismic events (Appendix A, B and C), and they create a restraining stepover, the Divriği Thrust (DvT), with the Ecemiş-Deliler Fault (EDF) (see below), providing a structural link between the CAFZ and NAFZ where the Erzincan Plain is located (Figures 1 and 2).

Northwest Margin of the Anatolian Diagonal: Its Relationship with the Cyprus Arc

There are several hypotheses about the link between the Aegean and Cyprus arcs. The suggestions of Biju-Duval et al. (1976) are among the oldest, connecting the arcs with a single line. Similarly, we propose here that the offshore continuation of Ecemiş-Deliler Fault (EDF) (Appendix A) is a possible candidate for separating structure between Aegean and Cyprus arcs together with the Antalya-Kekova Fault Zone (see below) (Figure 3). The Piri Reis (Mediterranean) Ridge Front turns from northeast to northwest 270 km south of eastern Crete (Morelli and Barrier, 2004; Yolsal-Çevikbilen and Taymaz, 2012). Although an intense deformation in the seismic reflection data of Huguen et al. (2001) is seen in the Seismic Lines-18 and -22, they can be regarded as deformation in the accretionary prism.

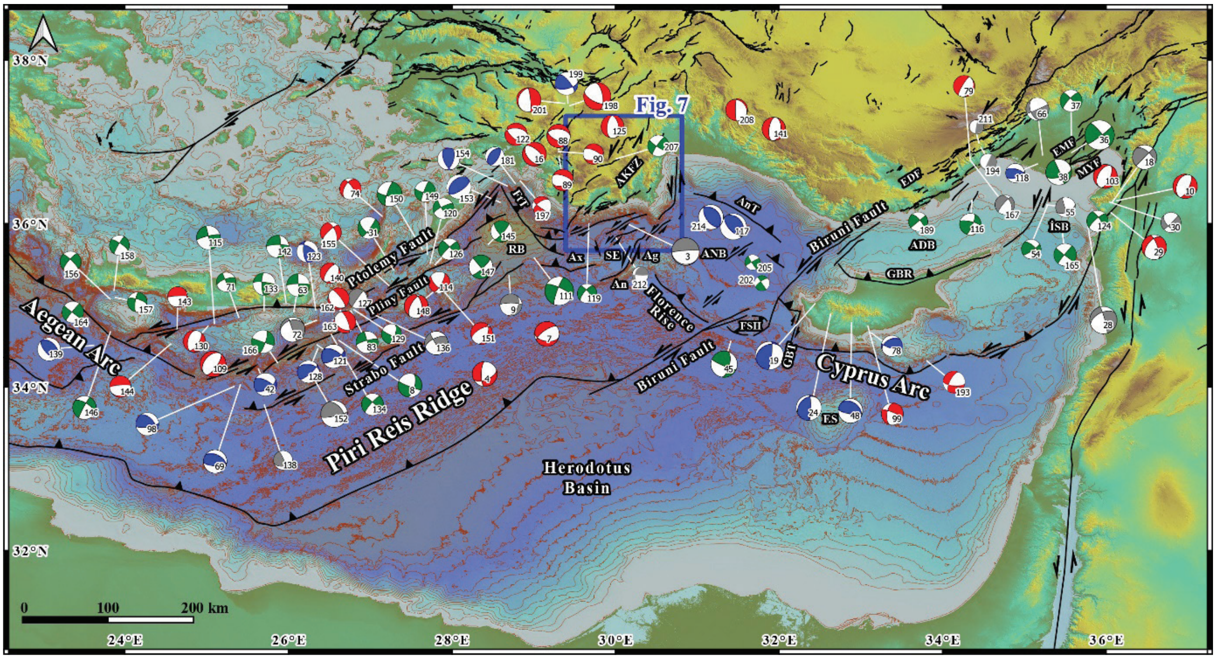

Figure 3. The role of Pliny-Strabo faults, Antalya-Kekova Fault Zone (AKFZ) and Biruni Fault of Anatolian Diagonal between the Aegean and Cyprus arcs. In the restraining stepovers, the Florence Rise and Antalya Thrust in the Antalya basin (ANB) and the Fethiye Thrust (FtT) in the NE margin of Rhodes basin (RB) developed. See Appendix B for details of focal mechanism solutions and Appendix A and C for details of faults. Fault lines are from Emre et al. (2013), Barrier et al. (2004), Seyitoğlu et al. (2022) and this paper. ES: Eratosthenes Mountain; GBT: Gazibaf Transform; FSH: Fuat Sezgin High; GBR: Girne-Beşparmak Range; ADB: Adana basin; EDF: Ecemiş-Deliler Fault; EMF: Elbistan-Misis Fault; MYF: Maraş-Yumurtalık Fault; İSB: İskenderun basin; AnT: Antalya Thrust; SE: Sırrı Erinç Plateau; Ax: Anaximander Mountain; Ag: Anaxagoras Mountain; An: Anaximenes Mountain.

***Şekil 3.** Ege ve Kıbrıs yayları arasında Anadolu Çaprazı'na ait Biruni Fayı, Antalya-Kekova Fay Zonu (AKFZ) ve Pliny-Strabo faylarının rolü. Daralmalı sıçrama alanlarında Antalya havzasında (ANB) Florence Yükselimi, Rodos havzası (RB) KD kenarında Fethiye bindirmesi (FtT) gelişmiştir. Odak mekanizması çözümleri için Appendix B'ye, Fayların detayları için Appendix A ve C'ye bakınız. Fay hatları Emre vd. (2013), Barrier vd. (2004), Seyitoğlu vd. (2022) ve bu makaleden alınmıştır.*

We suggest the name "Biruni Fault (BRF)" for the offshore continuation of the Ecemiş-Deliler Fault (EDF) which is concordant with the ancient geographers' names of the Pliny-Strabo faults in the region (Figure 3). South of Anamur, the segment locations of Biruni Fault (BRF-1, BRF-2, BRF-3) are determined using the seismic reflection profiles (Mansfield, 2005; Aksu et al., 2005) (Figure 4; e-suppl.-BRF in Appendix C). There is a pressure ridge named Fuat Sezgin High (FSH) west-southwest of Cyprus on the southeast tip of the Florence Rise (Figure 3). This pressure ridge possibly developed between the left-lateral segments of Biruni Fault (BRF). The north and south dipping thrusts were drawn by Woodside (1977, fig. 8), Woodside et al. (2002, fig. 7) and Güneş et al. (2018, Line-D, fig. 11). The segments of Biruni Fault (BRF) cut the Cyprus Arc, which is also displaced right-laterally by the Gazibaf (Paphos) Transform Fault west of Cyprus (Figure 3). The right-lateral nature of the Gazibaf Transform Fault (GBT) is determined by the focal mechanism solutions of recent earthquakes (Papazachos and Papaioannou, 1999; Yolsal-Çevikbilen and Taymaz, 2012).

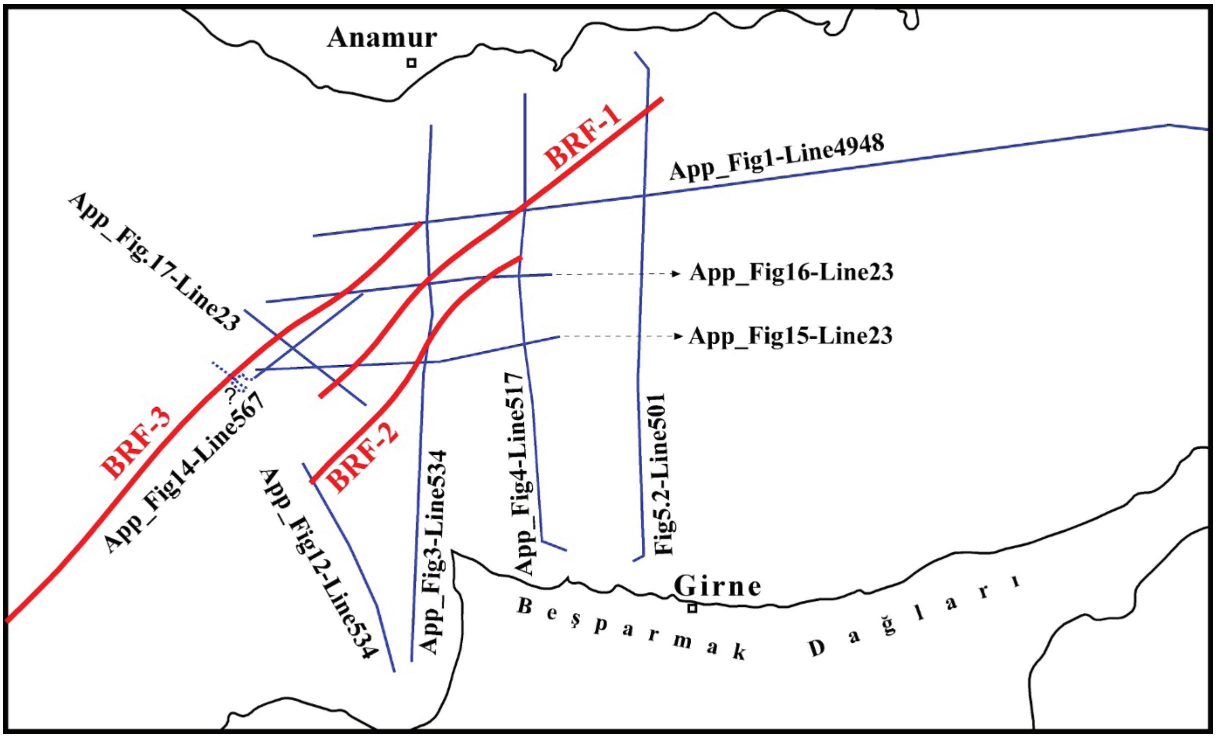

Figure 4. Locations of seismic reflection sections of Mansfield (2005) and segments of the Biruni Fault (BRF). The original names of the seismic lines are given on the map and this caption between quotation marks. The re-interpretation of seismic reflection data helps to locate the position of Biruni Fault. The southwest end of "App_ Fig14-Line 567" is not clear, therefore the position of yellow coloured BRF-3 has a question mark in e-suppl.-BRF in Appendix C. The NW-SE trending "App_Fig17-Line-23 contains segments BRF-3 and BRF-1 which were also marked by Mansfield (2005) as faults. The NW-SE trending "App_Fig12-Line-534 clearly shows segment BRF-2, recognized easily by the bathymetrical difference. The nearly E-W trending "App_Fig15-Line-23" indicates the positions of segments BRF-1 and BRF-2, with their typical negative flower structures. The N-S trending "Fig5.2-Line-501" has a strong positive flower structure near the coast of Anatolia marking the position of segment BRF-1. The flower structures are visible in the nearly E-W trending "App_Fig1-Line-4948" which are marked for the

location of segments BRF-3 and BRF-1. The nearly E-W trending "App_Fig16-Line-23 having negative flower structures, shows the positions of BRF-3 and BRF-2. BRF-1 marks the SW end of the bathymetrical trough visible on the Google Earth Image (see e-suppl.-BRF in Appendix C). A well-developed NE-SW trending trough visible on Google Earth Image corresponds to a negative flower structure in the N-S trending "App_Fig3-Line-534" marked with BRF-1. This NE-SW trending trough also provides a base to correlate fault traces diagonally. This seismic section is also used by Aksu et al. (2005) as Line-D. At least two possible fault locations exist on the N-S trending "App_Fig4-Line-517", marked as BRF-1 and BRF-2. See e-suppl.-BRF in Appendix C for the location information in the map view of the segments which are re-defined on each seismic section.

Şekil 4. *Mansfield (2005)'e ait sismik yansıma hatlarının konumu ve Biruni Fayı (BRF)'nın segmentleri. Sismik hatların orijinal isimleri haritada gösterilmiş olup, şekil alt yazısında tırnak içinde verilmiştir. Sismik yansıma kesitlerinin yeniden yorumlanması ile Biruni Fayı'nın konumu belirlenmiştir.*

Northwest Margin of the Anatolian Diagonal: The Re-Defined CAFZ

The segments of Biruni Fault (BRF) described above and its continuation onshore, the Ecemiş-Deliler Fault (EDF), expresses itself by developing linear valleys between Yanışlı and Taşucu. The segments of EDF create left-lateral shifting on Akdere and the course of Göksu River northwest and southeast of Silifke (Figure 5; Appendix A). Another important clue for the left-lateral strike-slip fault comes from the migration of the submarine delta of Göksu River (Aksu et al., 2014a, fig. 23). Moreover, in the offshore of Silifke, the seismic reflection lines of Okyar et al. (2005), Walsh-Kennedy et al. (2014), and Aksu et al. (2014a) indicate semi-parallel segments of the EDF. The epicenters of the seismic events # 116_2013.10.23 (M=4.5) and #189_2012.05.03 (M=4.0) are close to these segments and provide left-lateral focal mechanism solutions (Figure 5) (Appendix A, B, and C).

West - northwest of Mersin and Tarsus, the southeast slopes of the Taurus Mountains have several morphological indicators to locate segments of the EDF (Appendix A). This broad shear zone between Aydıncık and Gülek demonstrates that the Ecemiş-Deliler Fault (EDF) can safely be located on the Mediterranean coast (Figures 5 and 6; Appendix A).

Northeast of Gülek is where the Ecemiş Fault was originally defined, and called the Ecemiş corridor (Arpat and Şaroğlu, 1975; Yetiş, 1978) (Figure 6). Umhoefer et al. (2020) suggest that the Ecemiş corridor has a Late Eocene-Oligocene transpressional and post-Miocene transtensional character. Its spectacular morphological features were closely examined and dated recently by Sarıkaya et al. (2015) and Yıldırım et al. (2016), demonstrating late Quaternary activity in the Ecemiş Fault (Appendix A).

Further to the northeast, segments of the Ecemiş-Deliler Fault (EDF) create the Erciyes pull-apart basin (Dirik and Göncüoğlu, 1996; Koçyiğit and Beyhan, 1998) and a segment passing from the summit of Erciyes volcano (Emre et al., 2011b; Higgins et al., 2015) seems to behave as a cross basin fault (Figure 6; Appendix A, B, and C). The Ecemiş-Deliler Fault (EDF) has an ENE-WSW direction between Gemerek and Ulaş where Tuzla Gölü and Altınyayla Plain are two pull-apart structures (Figure 6). Finally, the Ecemiş - Deliler Fault (EDF) and Karaca Fault (KRF) create a restraining stepover where Divriği Thrust (DvT) is located (Figure 2; Appendix A, B, and C).

Internal Deformation of the Anatolian Diagonal

The internal deformation of Anatolian diagonal is accommodated by the Sarız (SZF), Ovacık (OVF), Malatya (MAF), Sürgü (SRF), Kantarma-Barış (KBF), Elbistan-Misis (EMF), Maraş-Yumurtalık (MYF) and Ayvalı (AYF) faults (Figures 2, 5 and 6).

The southwest end of left-lateral strike-slip Sarız Fault (SZF) creates a restraining stepover with the Ecemiş - Deliler Fault in Aladağlar where one of the highest summits in the region, Demirkazık (3756 m) is located. Its northeast end is closer to the Kemah-İliç Fault (KİF) east of Divriği Thrust (Figures 2 and 6) (Appendix A, B, and C).

The Ovacık Fault (OVF) is separated from the NAFZ south of Erzincan Plain. Its segments cut Quaternary alluvial fans west of Ovacık and created a distinguished left-lateral displacement on the course of Fırat River (Figure 2). The left lateral nature of Ovacık Fault (OVF) (Westaway and Arger, 2001; Yazıcı et al., 2018) is also confirmed by the focal mechanism solutions of the seismic events #110_2011.12.03 (M=4.0) and #135_2016.12.16 (M=4.4). The OVF constitutes the northwest margin of Kiğı rhomboidal cell and limits the Southeast Anatolian-Zagros Fault Zone (SAZFZ) (Seyitoğlu et al., 2018); while it ends with en echelon segments around Hekimhan which are responsible for the seismic events #131_2015.11.29 (M=4.9) and #200*_2019.03.25 (M=4.7) (Figure 2; Appendix A, B, and C).

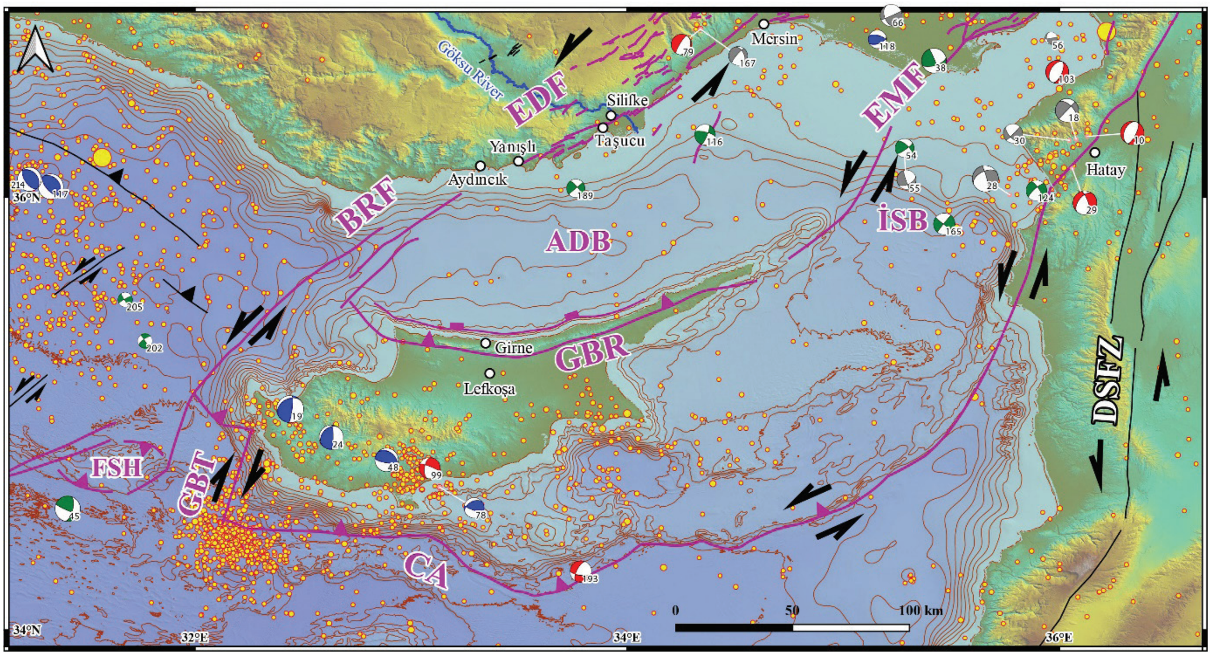

Figure 5. Southwest end of Anatolian Diagonal and its relationship with the Cyprus Arc. Fault lines are from Barrier et al. (2004), Emre et al. (2013), Symeou et al. (2018), Aksu et al. (2022) and this paper. See Appendix A and C for details of faults and Appendix B for focal mechanism solutions. The epicenter locations are from the ISC Catalogue (M≥3.5). BRF: Biruni Fault; EDF: Ecemiş-Deliler Fault; FSH: Fuat Sezgin High; EMF: Elbistan-Misis Fault; ADB: Adana Basin; İSB: İskenderun Basin; DSFZ: Dead Sea Fault Zone; GBR: Girne-Beşparmak Range; GBT: Gazibaf Transform; CA: Cyprus Arc.

Şekil 5. *Anadolu Çaprazı'nın güneybatı ucu ve Kıbrıs Yayı ile ilişkisi. Fay hatları Barrier vd. (2004), Emre vd. (2013), Symeou vd. (2018), Aksu vd. (2022) ve bu makale'den alınmıştır. Fayların detayları için Appendix A ve C'ye, odak mekanizmaları için Appendix B'ye bakınız. Dış merkez konumları ISC kataloğundan (M≥3,5) alınmıştır.*

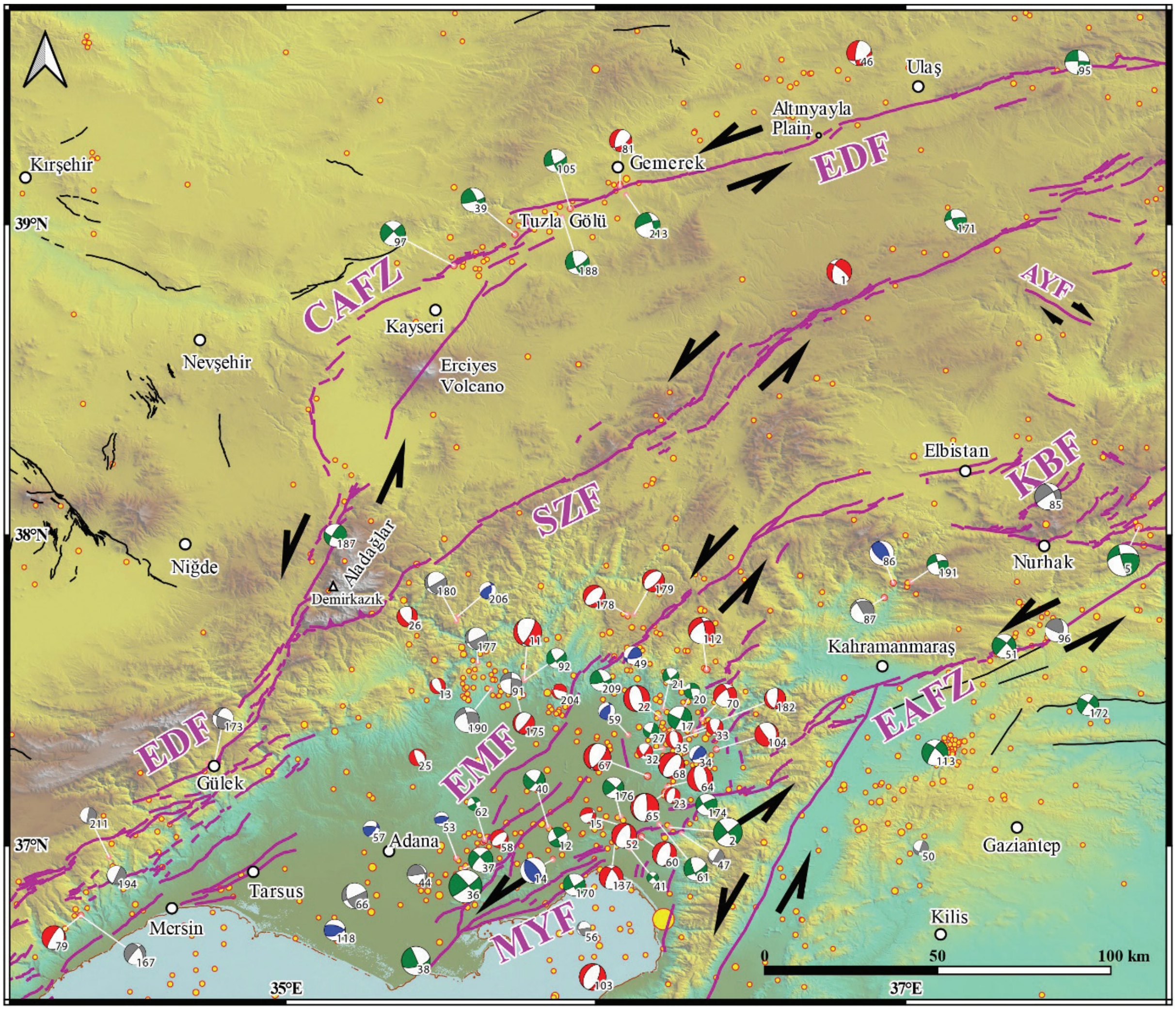

Figure 6. Anatolian Diagonal between Central Anatolian Fault Zone (CAFZ) and East Anatolian Fault Zone (EAFZ). Fault lines are from Emre et al. (2013), Seyitoğlu et al. (2017), and this paper. See Appendix A and C for details of faults and Appendix B for focal mechanism solutions. The epicenter locations are from the ISC Catalogue (M≥3.5). EDF: Ecemiş-Deliler Fault; SZF: Sarız Fault; EMF: Elbistan-Misis Fault; KBF: Kantarma-Barış Fault; MYF: Maraş-Yumurtalık Fault; AYF: Ayvalı Fault.

Şekil 6. *Orta Anadolu Fay Zonu (CAFZ) ile Doğu Anadolu Fay Zonu (EAFZ) arasında Anadolu Çaprazı'nın konumu. Fay hatları Emre vd. (2013), Seyitoğlu vd. (2017) ve bu makaleden alınmıştır. Fayların detayları için Appendix A ve C'ye, odak mekanizma çözümleri için Appendix B'ye bakınız. Dış merkez konumları ISC kataloğundan (M≥3,5) alınmıştır.*

The NNE-SSW trending segments of the left-lateral Malatya Fault (MAF) are located between the north of Arguvan and Nurhak (Figure 2). They nearly correspond to the R-shear in the Anatolian Diagonal, similar to the Kantarma-Barış Fault (KBF) (Figure 6) (Appendix A, B, and C). There is no agreement on the character of Sürgü Fault (SRF) among researchers (i.e., Koç and Kaymakçı, 2013; Emre et al., 2013), but the focal mechanism solutions of the seismic events #5_1986.05.05 (M=6.0) and #6_1986.06.06 (M=5.7) confirm its left-lateral strike-slip nature. The Sürgü Fault

(SRF) can be evaluated as P-shear in the Anatolian Diagonal (Figure 2; Appendix A, B and C).

The overall position of the Elbistan - Misis Fault (EMF) nearly corresponds to the R-shear in the Anatolian Diagonal and its segments create releasing stepovers where N-S normal faults developed, as seen in the east of Andırın, Yeşilova and Düziçi (Appendix A). Moreover, the Maraş-Yumurtalık Fault (MYF) is separated as a nearly parallel branch of the EAFZ and its segments create a releasing stepover where the N-S normal faults developed east of Osmaniye (Figure 6; Appendix A, B, and C).

The Ayvalı Fault (AYF) has been mapped as a NW-SE trending right-lateral strike-slip fault (Emre et al., 2012c). Its new semi-parallel segments demonstrate that the Anatolian Diagonal is a broad shear zone and the segments of Ayvalı Fault (AYF) are the right-lateral X-shears (Figures 2 and 6; Appendix A, B, and C).

ANTALYA-KEKOVA FAULT ZONE (AKFZ): A STRUCTURE BETWEEN THE ANATOLIAN DIAGONAL AND THE PLINY / STRABO / PTOLEMY FAULTS

The Biruni Fault (BRF) separates the Aegean and Cyprus arcs together with the Antalya-Kekova Fault Zone (AKFZ) (Figures 3 and 7). The position of BRF is defined by using the seismic lines of Mansfield (2005), Woodside et al. (2002), and Güneş et al. (2018). There is an important restraining stepover between the Biruni Fault (BRF) and the Antalya-Kekova Fault Zone (AKFZ) locating the western coast of Antalya Gulf (Figure 3).

The Antalya Fault has previously been proposed, but its character is controversial (Savaşçın et al., 1995; Barka and Reilinger, 1997; Aksu et al., 2014b; Hall et al. 2014a). While Aksu et al. (2014b) and Savaşçın et al. (1995) accepted that it is a right-lateral strike-slip fault, Barka and Reilinger (1997) draw the Antalya Fault as a left-lateral lineament (see also Hall et al. 2014a), with which we agree, because the Antalya Basin contains features of a restraining stepover which is represented by the NW-SE trending Antalya Thrusts having NNE-SSW trending left-lateral tear faults, as mapped by Güneş et al. (2018) (Figure 3; Appendix C).

The seismic reflection lines of Aksu et al. (2009, 2014b) and Güneş et al. (2018) offshore of Demre indicate NNE-SSW and NE-SW trending faults. Their semi-parallel counterparts onshore are mapped as the Kekova and Kale faults (Emre and Duman, 2011b) west of Demre (Figure 7; Appendix C).

We re-defined the segment distributions and examined the morphological features (i.e., distinctive displacement of stream channels, linear mountain-piedmont junctions) of the onshore faults and evaluated these faults as left-lateral strike-slip in nature. Especially the Ahatlı Fault presents a distinct linear morphology and a 5.70 km left-lateral displacement was measured on the Felenk Çayı. Moreover, semi-parallel faults between the northwest of Kaş and northeast of Korkuteli also have a distinctive morphology, where the focal mechanism solution of the #207*_2019.11.16 (Mw=4.4) Bozhüyük-Elmalı earthquake shows a NE-SW trending left-lateral faulting, but its deep hypocenter (69.5 km) creates a question mark about the evaluation (Figure 7; Appendix B and C).

We infer that the offshore counterparts seen in the seismic reflection sections must be of the same character. Indeed, examination of the published seismic sections shows that the majority of the fault lines could easily be re-evaluated as strike-slip faulting rather than thrusting (Aksu et al., 2009, 2014b; Güneş et al., 2018). This view is supported by the focal mechanism solution of seismic event #119_2014.03.24 (Mb=4.1) indicating that the nearest Finike Fault (FİN) is a left-lateral structure. As a conclusion, offshore and onshore data indicate that the Antalya, Finike, Kekova, Kaş, Demre, Çevreli, Yavu, Davazlar, Ahatlı, Bezirgan, Beldibi, Gömbe, Elmalı, Çobanisa, Korkuteli, and Döşemealtı faults constitute the left-lateral Antalya-Kekova Fault Zone (AKFZ) (Figure 7; Appendix B and C).

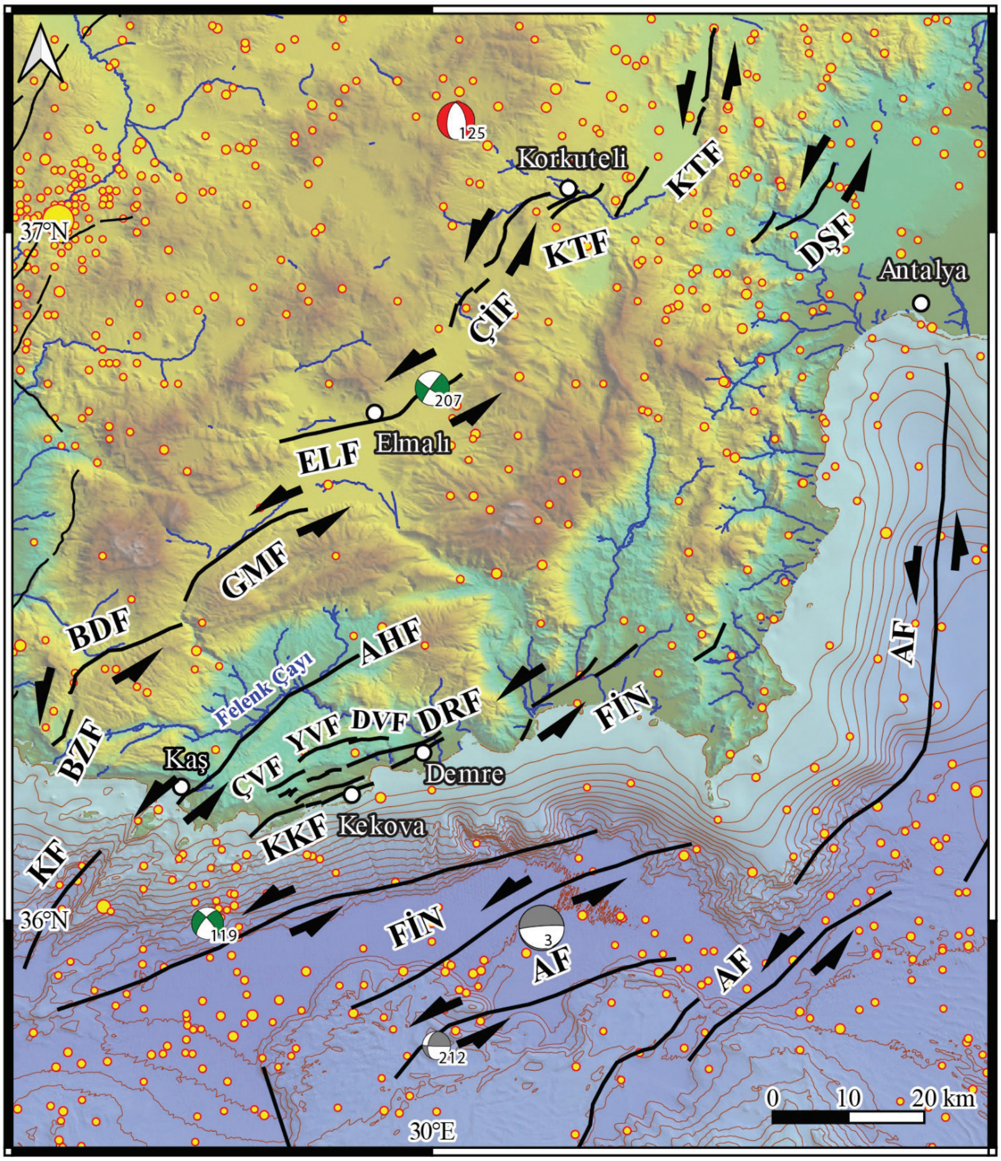

Figure 7. Offshore and onshore faults of Antalya-Kekova Fault Zone (AKFZ). Finike Fault (FİN) is taken from Aksu et al. (2009) and re-interpreted as a left-lateral strike-slip fault which is supported by the focal mechanism solution of seismic event #119. For focal mechanism solution see Appendix B, and for detail of the segment distribution, see Appendix C. KKF: Kekova Fault; DRF: Demre Fault; DVF: Davazlar Fault; AHF: Ahatlı Fault; KF: Kaş Fault; YVF: Yavu Fault; ÇVF: Çevreli Fault; BZF: Bezirgan Fault; BDF: Beldibi Fault; GMF; Gömbe Fault; ELF: Elmalı Fault. ÇİF: Çobanisa Fault; KTF: Korkuteli Fault; DŞF: Döşemealtı Fault.

Şekil 7. *Antalya-Kekova Fay Zonu (AKFZ)'na ait fayların karada ve deniz altındaki konumu. Finike Fayı (FİN) Aksu vd. (2009)'dan alınmış ve sol yanal doğrultu atımlı fay olarak yeniden yorumlanmıştır. Bu yorumu #119 numaralı depremin odak mekanizması çözümü desteklemektedir. Odak mekanizması çözümleri için Appendix B'ye, fayların detaylı segment dağılımı için Appendix C'ye bakınız.*

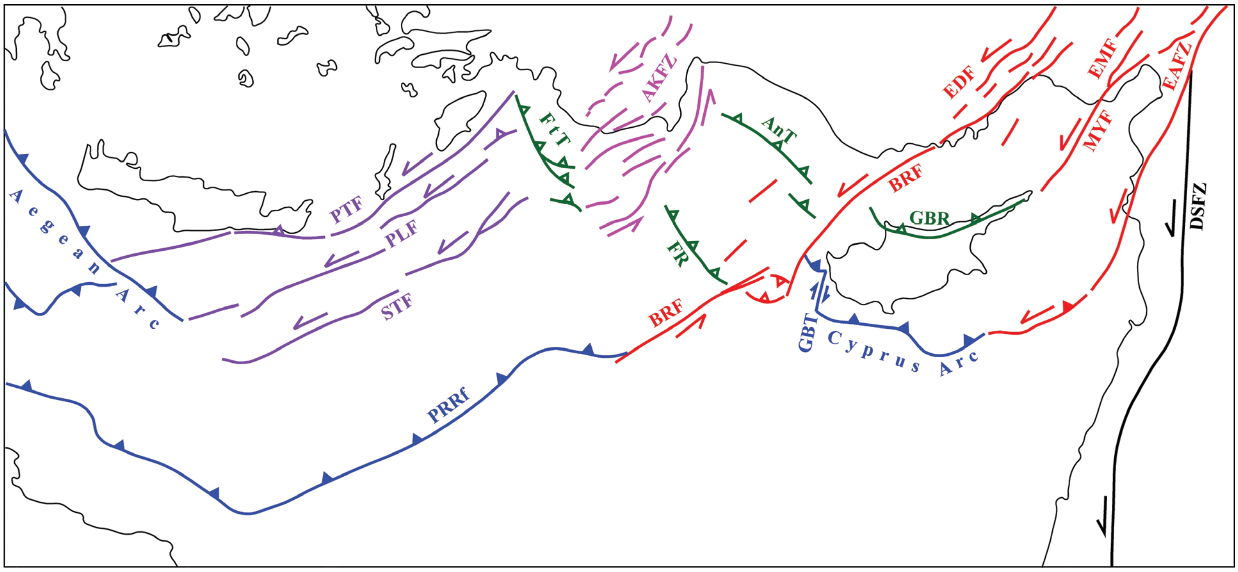

Figure 8. Schematic simplified drawing of relationship between the Aegean Arc, Cyprus Arc (blue) and Anatolian Diagonal Shear Zone (red), Antalya-Kekova Fault Zone (AKFZ) (fuchsia), and Ptolemy-Pliny-Strabo faults (purple). Note that the restraining stepovers (green) (i.e., AnT: Antalya Thrust; FR: Florence Rise FtT: Fethiye Thrust) developed between the right-stepping left-lateral shear zones. DSFZ: Dead Sea Fault Zone; EAFZ: East Anatolian Fault Zone; GBR: Girne-Beşparmak Range; MYF: Maraş-Yumurtalık Fault; EMF: Elbistan-Misis Fault; EDF: Ecemiş-Deliler Fault; BRF: Biruni Fault; GBT: Gazibaf Transform; PRRf: Piri Reis Ridge Front; PTF: Ptolemy Fault; PLF: Pliny Fault; STF: Strabo Fault.

Şekil 8. *Ege Yayı, Kıbrıs Yayı (mavi) ile Anadolu Çaprazı Makaslama Zonu (kırmızı), Antalya-Kekova Fay Zonu (AKFZ) (fuşya), Ptolemy-Pliny-Strabo fayları (mor) arasındaki ilişkiyi gösteren şematik basitleştirilmiş çizim.*

DISCUSSION

Relationship of the Anatolian Diagonal with the Aegean and Cyprus Arcs

The Biruni Fault (BRF) provides a structural link between the Piri Reis Ridge Front and the Cyprus Arc, and the Antalya-Kekova Fault Zone (AKFZ) creates a restraining stepover in which the Antalya Thrust and Florence Rise developed (Figures 3 and 8).

The position of the Antalya Thrust is based on the seismic reflection sections of Dündar and Varol (2019, fig. 12) and Güneş et al. (2018, fig. 6), which corresponds to the Aksu-Kyrenia Fault of Aksu et al. (2022, fig. 19). The seismic reflection presented in Aksu et al. (2022, fig. 13) can be easily re-interpreted as thrust-related structures such as ramp anticlines and back thrusts rather than normal faulting. This interpretation is concordant with the thrusts observed in Dündar and Varol (2019), Güneş et al. (2018), and Hall et al. (2014a, fig. 13).

The Florence Rise is evaluated as a NW-SE trending right-lateral transpressive wrench fault (Woodside et al., 2002; Zitter et al., 2003) or a left-lateral transpressive strike-slip fault, which creates a restraining bend south of Cyprus (Harrison et al., 2012). However, other studies evaluate the Florence Rise as a southwest verging thrust-related structure (Sage and Letouzey, 1990; Sellier et al., 2013a, b; Güneş et al., 2018). Howell et al. (2017) suggest that relatively deep thrust-related earthquakes (40-50 km) (i.e., seismic events #177_2013.12.28, M=5.5; #214_2022.01.05, M=5.0, Appendix B) occur in the subduction interface between Nubia and Anatolia, and the Florence Rise is interpreted as thickened sediments at the surface projection of this subduction interface. Recent evaluation of the Florence Rise as a forearc high or accretionary prism due to subduction of the Antalya slab also exists (Güvercin et al., 2021). On the other hand, it is not clear whether the trench of the subduction is just south of the Florence Rise or further southwest between Piri Reis Ridge front and Herodotus basin. For this reason, we infer that the Antalya Thrust and Florence Rise structures are related to the restraining stepover between the Biruni Fault and the Antalya-Kekova Fault Zone rather than subduction-related structures because their onshore counterparts such as the post-Late Pliocene Aksu Thrust (Poisson et al., 2003) also exists (Figures 3 and 8).

There is another contractional stepover between the Antalya-Kekova Fault Zone (AKFZ) and the Pliny / Strabo faults (Shaw and Jackson, 2010; Özbakır et al., 2013) where the thrust controlled northern margin of the Rhodes basin developed (Figures 3 and 8). This fault configuration can be confirmed by the focal mechanism solutions of the recent earthquakes (i.e., seismic event #154_2019.10.24, M=4.6, Appendix B) and by the geological cross sections of Aksu et al. (2009, fig. 26) and Hall et al. (2009, fig. 23). The seismic reflection data clearly show that the western margin of Rhodes basin is also controlled by a thrust, probably having a left-lateral strike-slip component (Woodside et al., 2000, fig.6) (Figures 3 and 8).

If the fault configuration explained above is correct, then there is no need for the Fethiye-Burdur Fault Zone, which is regarded as an onshore continuation of the Pliny and Strabo faults. Debate continues regarding the existence of the left-lateral Fethiye-Burdur Fault Zone (i.e., Hall et al., 2014b; Elitez and Yaltırak, 2016; Elitez et al., 2016; Howell et al., 2017; Kaymakçı et al., 2018; Özkaptan et al., 2018). Some researchers have argued that there is no seismic activity to demonstrate such a left-lateral shear zone in the southwest of Türkiye (Jackson et al., 2019; Howell et al., 2017), and the focal mechanism solutions of the main event and aftershocks of the recent Acıpayam earthquake (2019.03.20, Mw=5.5) (Çıvgın et al., 2019) are also not compatible with the left-lateral shearing.

In this case, the entire southwesterly motion of Anatolia indicated by the GPS results (Reilinger et al., 2006) must be accommodated by the Anatolian Diagonal Shear Zone and the Antalya-Kekova Fault Zone. This result also creates some question marks on the seismic evaluation of the Akkuyu Nuclear Power Plant Station (ANPPS) located on the Ecemiş-Deliler Fault (EDF) and the Biruni Fault (BRF), which creates an FFT triple junction with the Cyprus Arc (Figures 3 and 8).

Relationship of the Anatolian Diagonal with the NAFZ and SAZFZ

The Anatolian Diagonal is a left-lateral shear zone separating east / southeast Anatolia from central Anatolia. A recent neotectonic study (Seyitoğlu et al., 2017) in the foreland of the Bitlis-Zagros Suture Zone (BZSZ) suggests that the Southeast Anatolian Wedge (SEAW), consisting of blind thrusts, fault propagation folds and tear faults, is operational between the suture zone and the Sincar Mountains (Figure 1). The overall structure in the hinterland of BZSZ, however, is explained by the rhomboidal cells surrounded by left- and right-lateral strike-slip faults (Seyitoğlu et al., 2018). The southwest margins of the rhomboidal cells are aligned in a single line that creates region-wide shear zones. The most spectacular ones are the NAFZ and the SAZFZ (Figures 1 and 9).

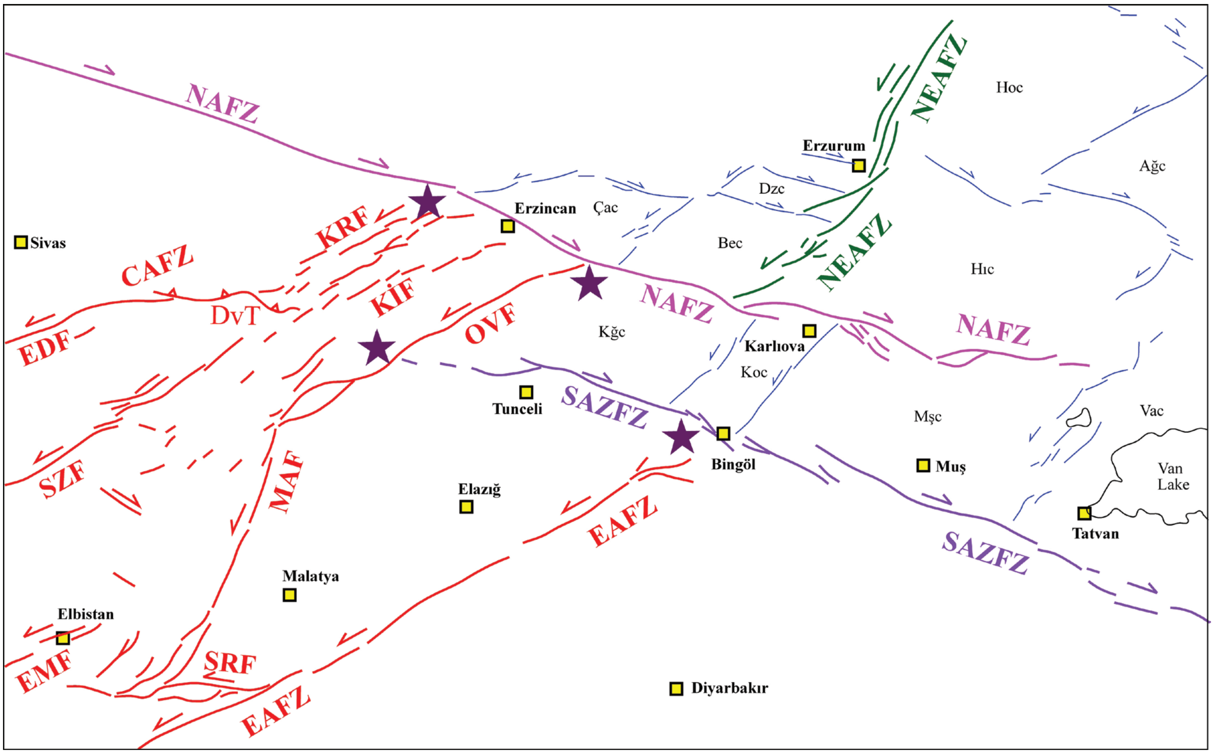

Figure 9. Schematic simplified drawing of the multiple intersection points (stars) between the right-lateral NAFZ (fuchsia) / SAZFZ (purple) and left-lateral Anatolian Diagonal Shear Zone (red). NAFZ: North Anatolian Fault Zone; NEAFZ: Northeast Anatolian Fault Zone; SAZFZ: Southeast Anatolian-Zagros Fault Zone; EAFZ: East Anatolian Fault Zone; CAFZ: Central Anatolian Fault Zone; SRF: Sürgü Fault; EMF: Elbistan-Misis Fault; MAF: Malatya Fault; OVF: Ovacık Fault; KİF; Kemah-İliç Fault; KRF: Karaca Fault; DvT: Divriği Thrust; EDF: Ecemiş_ Deliler Fault; SZF: Sarız Fault. The rhomboidal cells (blue) are of Seyitoğlu et al. (2018), Çac: Çayırlı cell; Dzc: Düzyurt cell; Bec: Beşgöze cell; Hoc: Horasan cell; Hıc: Hınıs cell; Ağc: Ağrı cell; Vac: Van cell; Mşc: Muş cell; Koc: Karlıova cell; Kğc: Kiğı cell.

Şekil 9. *Sağ yanal Kuzey Anadolu Fay Zonu (fuşya) / Güneydoğu Anadolu-Zagros Fay Zonu (mor) ile sol yanal Anadolu Çaprazı (kırmızı) arasındaki çoklu kesişim noktalarını (yıldızlar) gösteren şematik basitleştirilmiş çizim.*

The NAFZ does not terminate at Karlıova, as previously suggested; to the contrary, it continues southeast along the Varto Fault (Seyitoğlu et al., 2018) (Figure 9). The NAFZ connects with the Anatolian Diagonal and a newly-recognized intersection point of these two structures is the Erzincan Plain (Figure 9), where the Karaca Fault (KRF) represents the northwest margin of the Anatolian Diagonal Shear Zone. The Karaca (KRF) and Kemah - İliç (KİF) faults link to the Ecemiş-Deliler Fault (EDF) with a restraining bend where the Divriği Thrust (DvT) developed (Figure 9). The Kemah-İliç Fault (KİF) also links with the right stepping Sarız Fault (SZF). The Ovacık Fault (OVF), the northwest margin of Kiğı rhomboidal cell (Seyitoğlu et al., 2018), limits the Nazimiye Fault of the SAZFZ. In other words, the Anatolian Diagonal Shear Zone limits the SAZFZ west of Tunceli (Figure 9).

In Bingöl, there is an intersection point between the right-lateral SAZFZ and the left-lateral EAFZ where NNE-SSW contraction takes place (Seyitoğlu et al., 2018). The overall fault configuration in the region creates a complex relationship between the left-lateral Anatolian Diagonal Shear Zone and the right-lateral NAFZ and SAZFZ (Figure 9). It is not a simple case as explained earlier in the tectonic escape model, which proposes a single intersection point between the right- and left-lateral structures (Şengör et al., 1985, 2019). Instead, multiple intersection points exist between the left-lateral Anatolian Diagonal Shear Zone and the right-lateral NAFZ and the SAZFZ (Figure 9).

The area of Sivas-Yozgat-Kırşehir moves towards the southwest as a block (internal deformation of this block can be ignored at this stage for the sake of simplicity) between the left-lateral Karaca (KRF) and Ecemiş-Deliler (EDF) faults of the Anatolian Diagonal Shear Zone and the right-lateral Kırıkkale-Erbaa Fault Zone (KEFZ) (Şengör et al., 1985; Seyitoğlu et al., 2009) (Figure 1). The southwest movement of this block must be slower than the rest of southwest Türkiye, otherwise we could not observe the normal fault-related earthquakes on the Sultandağları Fault Zone (Akyüz et al., 2006b; Kaya et al., 2014) (Figure 1).

CONCLUSIONS

The Anatolian Diagonal is a 170 km wide left-lateral shear zone developed between the EAFZ and the CAFZ and it extends from Erzincan to the Cyprus Arc for 850 km. The internal deformation of the shear zone is accommodated by the major structures such as Ovacık, Malatya, Sürgü, Kantarma-Barış, Elbistan- Misis, Maraş-Yumurtalık and Ayvalı faults. The relationship between the right-lateral NAFZ / SAZFZ and the left-lateral Anatolian Diagonal is so complex that it cannot be explained with a single intersection point at Karlıova, as previously proposed. At least four intersection points exist between the right-lateral NAFZ / SAZFZ and the left-lateral Anatolian Diagonal Shear Zone (Figure 9). The first intersection point is Erzincan Plain where the NAFZ connects to the Anatolian Diagonal and causes west-southwest translation of the Sivas-Yozgat-Kırşehir block. The second intersection is southeast of Erzincan Plain where the NAFZ and the Ovacık Fault (OVF) meet. The third intersection is west-northwest of Tunceli where the Anatolian Diagonal (Ovacık Fault) limits the SAZFZ. The fourth intersection occurs in Bingöl where the SAZFZ cuts the EAFZ of the Anatolian Diagonal (Figure 9). In this area, it should also be noted that the NAFZ and the SAZFZ have a releasing stepover where Kiğı, Karlıova, and Muş rhomboidal cells developed (Seyitoğlu et al., 2018) (Figure 9).

The southwest ends of the left-lateral faults belonging to the Anatolian Diagonal cut and/or merge with the Cyprus Arc and the EAFZ connects to the Cyprus Arc. The Maraş-Yumurtalık Fault (MYF) connects the Anatolian Diagonal to the Girne-Beşparmak Range (GBR) (Kyrenia Range) (Figure 8). More importantly, the southwest continuation of the Ecemiş-Deliler Fault (EDF) reaches the Mediterranean coast. Its extension under the Mediterranean Sea, the Biruni Fault (BRF), is observed in the seismic reflection data. The Biruni Fault (BRF) cuts the Cyprus Arc and creates a TFF triple junction west of Cyprus (Figure 8).

The right stepping of the left-lateral Antalya-Kekova Fault Zone (AKFZ) creates a restraining stepover in the Antalya basin where the Florence Rise and Antalya Thrusts are visible in the seismic reflection sections. There is another restraining stepover between the Antalya-Kekova Fault Zone and the Pliny / Strabo faults where thrusts are predicted on the northern margin of Rhodes basin due to the recent thrust-related earthquakes (i.e., #154_2019.10.24, M=4.6; and #153_2019.10.03, M=5.1) (Figures 3 and 8).

GENİŞLETİLMİŞ ÖZET

Anadolu Çaprazı, Doğu Anadolu Fay Zonu ile Orta Anadolu Fay Zonu arasında 170 km genişliğe ve Erzincan ile Kıbrıs Yayı arasında 850 km uzunluğa sahip sol yanal makaslama zonudur (Şekil 1). Bu makaslama zonunun iç deformasyonu Ovacık, Malatya, Sürgü, Kantarma-Barış, Elbistan-Misis, Maraş-Yumurtalık ve Ayvalı fayları gibi ana yapılar tarafından karşılanır. Sağ yanal Kuzey Anadolu Fayı / Güneydoğu Anadolu – Zagros Fay Zonu ve sol yanal Anadolu Çaprazı arasındaki ilişki oldukça karmaşıktır ve daha önce öne sürüldüğü gibi Karlıova'da tek bir kesişim noktası ile açıklanamaz. Sağ yanal Kuzey Anadolu Fay Zonu / Güneydoğu Anadolu – Zagros Fay Zonu ile sol yanal Anadolu Çaprazı arasında en az dört kesişim noktası bulunur (Şekil 9). İlk kesişim noktası Erzincan Ovasında olup, burada Kuzey Anadolu Fay Zonu ve Anadolu Çaprazı bir araya gelerek Sivas-Yozgat-Kırşehir bloğunun batı-güneybatı hareketine neden olur. İkinci kesişim noktası Erzincan ovasının güneydoğusunda olup, burada Kuzey Anadolu Fay Zonu ve Ovacık Fayı bir araya gelmektedir. Üçüncü kesişim noktası Tunceli'nin batı – kuzeybatısında olup, burada Anadolu Çaprazına ait Ovacık Fayı Güneydoğu Anadolu-Zagros Fay Zonu'nu sonlandırır. Dördüncü kesişim noktası Bingöl'de olup, burada Güneydoğu Anadolu-Zagros Fay Zonu, Anadolu Çaprazına ait Doğu Anadolu Fay Zonu'nu keser (Şekil 9). Bu alanda Kuzey Anadolu Fay Zonu ve Güneydoğu Anadolu – Zagros Fay Zonu rahatlamalı bir sıçrama yapmakta olup, burada Kiğı, Karlıova, ve Muş eşkenar dörtgen benzeri hücreler gelişmiştir (Seyitoğlu vd. 2018) (Şekil 9).

Anadolu Çaprazına ait sol yanal fayların güneybatı uçları Kıbrıs Yayı'na bağlanır ve/veya keserler. Doğu Anadolu Fay Zonu Kıbrıs Yayına bağlanmaktadır. Maraş-Yumurtalık Fayı, Anadolu Çaprazı'nı Girne -Beşparmak Sırtı'na bağlar (Şekil 8). Daha önemlisi, Ecemiş-Deliler Fayı'nın güneybatı devamı Akdeniz kıyısına ulaşır. Bunun Akdeniz'deki devamı olan ve sismik yansıma kesitlerinde gözlenen Biruni Fayı Kıbrıs Yayı'nı keserek Kıbrıs batısında TFF üçlü eklemini oluşturur (Şekil 8).

Antalya-Kekova Fay Zonu'nun sağa sıçraması Antalya havzasında daralmalı sıçrama meydana getirir, burada Florence Yükselimi ve Antalya bindirmeleri sismik yansıma kesitlerinde izlenebilmektedir. Diğer bir daralmalı sıçrama Antalya-Kekova Fay Zonu ile Pliny/Strabo Fayları arasında gelişmiştir. Burada Rodos havzasının kuzey kenarında gelişmiş bindirmeler yer almakta olup, yakın zamanda bindirmeler ile ilişkili depremler meydana gelmiştir (örn., #154_2019.10.24, M=4,6; #153_2019.10.03, M=5,1) (Şekiller 3 ve 8).

ELECTRONIC APPENDIX A

Link 1: https://dergipark.org.tr/tr/download/issue-file/56855

Link 2: https://www.jmo.org.tr/resimler/ekler/9ef73dd7ef07bf3_ek.pdf

ELECTRONIC APPENDIX B

Link 1: https://dergipark.org.tr/tr/download/issue-file/56856

Link 2: https://www.jmo.org.tr/resimler/ekler/6f8d8e1e8fd822f_ek.pdf

ELECTRONIC APPENDIX C

Link 1: https://www.jmo.org.tr/resimler/ekler/8488de0d69c136b_ek.rar

ORCID

Gürol Seyitoğlu https://orcid.org/*0000-0001-7993-898X*

Esra Tunçel https://orcid.org/0000-0001-7434-4111

Bülent Kaypak https://orcid.org/0000-0003-4650-9171

Korhan Esat https://orcid.org/0000-0003-2592-9281

Ergin Gökkaya https://orcid.org/0000-0002-9808-6708

REFERENCES / *KAYNAKLAR*

Acarel, D., Cambaz, M. D., Turhan, F., Mutlu, A. K. & Polat, R. (2019). Seismotectonics of Malatya Fault, Eastern Turkey. *Open Geosciences, 11*, 1098-1111.

Aksu, A. E., Calon, T. J., Hall, J., Mansfield, S. & Yaşar, D. (2005). The Cilicia–Adana basin complex, Eastern Mediterranean: Neogene evolution of an active fore-arc basin in an obliquely convergent margin. *Marine Geology, 221*, 121-159.

Aksu, A. E., Hall, J. & Yaltırak, C. (2009). Miocene–Recent evolution of Anaximander Mountains and Finike Basin at the junction of Hellenic and Cyprus Arcs, eastern Mediterranean. *Marine Geology, 258*, 24-47.

Aksu, A. E., Walsh-Kennedy, S., Hall, J., Hiscott, R.N., Yaltırak, C., Akhun, S.D. & Çifçi, G. (2014a). The Pliocene–Quaternary tectonic evolution of the Cilicia and Adana basins, eastern Mediterranean: Special reference to the development of the Kozan Fault zone. *Tectonophysics, 622*, 22-43.

Aksu, A. E., Hall, J., Yaltırak, C., Çınar, E., Küçük, M. & Çifçi, G. (2014b). Late Miocene-Recent evolution of the Finike basin and its linkages with the Beydağları complex and the Anaximander Mountains, eastern Mediterranean. *Tectonophysics, 635*, 59-79.

Aksu, A. E., Hall, J. & Yaltırak, C. (2022). The uppermost Messinian-Quaternary evolution of the Anamur-Kormakiti zone: The transition between the Outer Cilicia and Antalya basins. *Marine and Petroleum Geology, 136*, 105451.

Akyüz, H. S., Altunel, E., Karabacak, V. & Yalçıner, C. Ç. (2006a). Historical earthquake activity of the northern part of the Dead Sea Fault Zone, southern Turkey. *Tectonophysics, 426*, 281-293.

Akyüz, H. S, Uçarkuş, G., Şatir, D., Dikbaş, A. & Kozacı, Ö. (2006b). 3 Şubat 2002 Çay depreminde meydana gelen yüzey kırığı üzerinde paleosismolojik araştırmalar. *Yerbilimleri, 27*, 41-52.

Alan, İ., Balcı, V. & Elibol, H. (2014.) *Geological map of the Silifke-P31 and P32 Quadrangles*. MTA-Ankara, Türkiye.

Arpat, E. & Şaroğlu, F. (1972). The East Anatolian fault system; thoughts on its development. *Bulletin of the Mineral Research and Exploration, 78*, 33-39.

Arpat, E. & Şaroğlu, F. (1975). Türkiye'deki bazı önemli genç tektonik olaylar. *Türkiye Jeoloji Kurumu Bülteni, 18*, 91-101. http://tjb.jmo.org.tr/detail-article.php?articlekod=63

Barka, A. A. & Reilinger, R. (1997). Active tectonics of the Mediterranean region: Deduced from GPS, neotectonic and seismicity data. *Annales Geofisica, 40*, 587-610.

Barrier, E., Chamot Rooke, N. & Giordano, G. (2004). *Geodynamic Maps of the Mediterranean-sheet 1: Tectonics and Kinematics*. Commission for the Geological map of the World (CGMW) and UNESCO.

Biju-Duval, B., Dercourt, J. & Le Pichon, X. (1976). From the Tethys Ocean to the Mediterranean Seas: A plate tectonic model of the evolution of the western Alpine system. In B. Biju-Duval, L. Montadert, (Eds.), *International Symposium on the Structural History of the Mediterranean Basins, Split (Yugoslavia)*, (p. 143-164). Editions Technip Paris

Chorowicz, J., Dhont, D. & Gündoğdu, N. (1999). Neotectonics in the eastern North Anatolian Fault region (Turkey) advocates crustal extension: mapping from SAR ERS imagery and Digital Elevation Model. *Journal of Structural Geology, 21*, 511-532.

Çıvgın, B., Kaypak, B., Seyitoğlu, G., Aktuğ, B., Kılıçarslan, Ö. & Akkoyunlu, F. (2019). An approach to the tectonic structure of the Acıpayam Basin: Analysis of the 20.03.2019 (Mw 5.5) earthquake and its aftershocks. *20th Anniversary of the 1999 Marmara Earthquakes: 23rd Active Tectonics Research Group Meeting, Abstract Books*, İstanbul, Türkiye.

Davis, P. (1971). Distribution patterns in Anatolia with particular reference to endemism. In P. H. Davis & I. C. Hedge (Eds.), *Plant life of southwest Asia* (pp. 15-28). University Press, Aberdeen.

Dirik, K. & Göncüoğlu, M. C. (1996). Neotectonic characteristics of central Anatolia. *International Geology Reviews, 38*, 807-817.

Dirik, K., Yürür, T. & Demirbağ, H. (2003). *1 Mayıs 2003 Çimenli (Bingöl) Depremi Değerlendirme Raporu*. https://www.doi.org/10.13140/2.1.5130.1449

Duman, T. Y. & Emre, Ö. (2013). The East Anatolian Fault: geometry, segmentation and jog characteristics. *Geological Society London Special Publications, 372*, 495-529.

Dündar, S. & Varol, B. (2019). New insights on Messinian evaporites based on field and seismic interpretations in the Neogene Antalya Basin, SW Turkey. *Turkish Journal of Earth Sciences, 28*, 687-705.

Dziewonski, A. M., Chou, T-A. & Woodhouse, J. H. (1981). Determination of earthquake source parameters from waveform data for studies of global and regional seismicity. *Journal of Geophysical Research, 86*, 2825-2852.

Ekström, G., Nettles., M. & Dziewonski, A. M. (2012). The global CMT project 2004-2010: Centroid-moment tensors for 13,017 earthquakes. *Physics of the Earth Planetary Interiors*, *200-201*, 1-9.

Elitez, İ. & Yaltırak, C. (2016). Miocene to Quaternary tectonostratigraphic evolution of the middle section of the Burdur – Fethiye Shear Zone, south-western Turkey: Implications for the wide inter-plate shear zones. *Tectonophysics, 690*, 336-354.

Elitez, İ., Yaltırak, C. & Aktuğ, B. (2016). Extensional and compressional regime driven left-lateral shear in southwestern Anatolia (eastern Mediterranean). The Burdur – Fethiye Shear Zone. *Tectonophysics, 688*, 26-35.

Emre, Ö. & Duman, T. (2011a). *1:250,000 Scale active fault map series of Turkey, Mersin (NJ 36-16) Quadrangle Serial Number: 34.* General Directorate of Mineral Research and Exploration, Ankara-Turkey.

Emre, Ö. & Duman, T. (2011b). *1:250,000 Scale active fault map series of Turkey, Fethiye (NJ 35-16) Quadrangle Serial Number: 13*. General Directorate of Mineral Research and Exploration, Ankara-Turkey.

Emre, Ö., Duman, T., Özalp, S., Elmacı, H. & Olgun, Ş. (2011a). *1:250,000 Scale active fault map series of Turkey, Adana (NJ 36-12) Quadrangle Serial Number: 33*. General Directorate of Mineral Research and Exploration, Ankara-Turkey.

Emre, Ö., Duman, T., Özalp, S., Elmacı, H. & Olgun, Ş. (2011b). *1:250,000 Scale active fault map series of Turkey, Kayseri (NJ 36-8) Quadrangle Serial Number: 32*. General Directorate of Mineral Research and Exploration, Ankara-Turkey.

Emre, Ö., Duman, T., Olgun, Ş., Elmacı, H. & Özalp, S. (2012a). *1:250,000 Scale active fault map series of Turkey, Divriği (NJ 37-2) Quadrangle Serial Number: 41*. General Directorate of Mineral Research and Exploration, Ankara-Turkey.

Emre, Ö., Duman, T. Y., Elmacı, H., Özalp, S. & Olgun, Ş. (2012b). *1:250,000 Scale active fault map series of Turkey, Malatya (NJ37-6) Quadrangle Serial Number: 42*. General Directorate of Mineral Research and Exploration, Ankara-Turkey.

Emre, Ö., Duman, T. & Elmacı, H. (2012c). *1:250,000 Scale active fault map series of Turkey, Elbistan (NJ 37-5) Quadrangle. Serial Number: 37*. General Directorate of Mineral Research and Exploration, Ankara-Turkey.

Emre, Ö., Duman, T., Olgun, Ş., Elmacı, H. & Özalp, S. (2012d). *1:250,000 Scale active fault map series of Turkey, Gaziantep (NJ 37-9) Quadrangle Serial Number: 38*. General Directorate of Mineral Research and Exploration, Ankara-Turkey.

Emre, Ö., Duman, T., Özalp, S., Elmacı, H., Olgun, Ş. & Şaroğlu, F. (2013). *Active fault map of Turkey with and explanatory text. Special Publication Series 30*. General Directorate of Mineral Research and Exploration, Ankara-Turkey.

Emre, Ö., Duman, T. Y., Özalp, S., Şaroğlu, F., Olgun, Ş., Elmacı, H. & Çan, T. (2018). Active fault database of Turkey. *Bulletin of Earthquake Engineering, 16*, 3229-3275.

Ergin, M. (1999). *Present day seismicity and seismotectonic characteristics of the Cilician region* [Unpublished PhD thesis]. Istanbul Technical University.

Ergin, M., Aktar, M. & Eyidoğan, H. (2004). Present-Day Seismicity and Seismotectonics of the Cilician Basin: Eastern Mediterranean Region of Turkey. *Bulletin of the Seismological Society of America, 94*, 930-939.

Esri (2021). "Ocean" [basemap]. Scale Not Given. "World Ocean Base". January, 2021. https://server.arcgisonline.com/arcgis/rest/services/Ocean/World_Ocean_Base/MapServer (January, 2022).

Güneş, P., Aksu, A. E. & Hall, J. (2018). Structural framework and deformation history of the western Cyprus Arc. *Tectonophysics, 744*, 438-457.

Güvercin, S. E., Konca, A. Ö., Özbakır, A. D., Ergintav, S. & Karabulut, H. (2021). New focal mechanisms reveal fragmentation and active subduction of the Antalya slab in the Eastern Mediterranean. *Tectonophysics 805*, Article 228792. doi.org/10.1016/j.tecto.2021.228792.

Hall, J., Aksu, A. E., Yaltırak, C. & Winsor, J. D. (2009). Structural architecture of the Rhodes Basin: A deep depocentre that evolved since the Pliocene at the junction of Hellenic and Cyprus Arcs, eastern Mediterranean. *Marine Geology, 258*,1-23.

Hall, J., Aksu, A. E., King, H., Gogacz, A., Yaltırak, C. & Çifçi, G. (2014a). Miocene–Recent evolution of the western Antalya Basin and its linkage with the Isparta Angle, eastern Mediterranean. *Marine Geology, 349*, 1-23.

Hall, J., Aksu, A. E., Elitez, I., Yaltırak, C. & Çifçi, G. (2014b). The Fethiye-Burdur Fault Zone: A component of upper plate extension of the subduction transform edge propagator fault linking Hellenic and Cyprus Arcs, Eastern Mediterranean. *Tectonophysics, 635*, 80-99.

Harrison, R.W., Tsiolakis, E., Stone, B.D., Lord, A., McGheehin, J. P., Mahan, S. A. & Chirico, P. (2012). Late Pleistocene and Holocene uplift history of Cyprus: implications for active tectonics along the southern margin of the Anatolian microplate. In A.H.F. Robertson, O. Parlak & U.C. Ünlügenç, (Eds.), *Geological Development of Anatolia and the Easternmost Mediterranean Region*. Geological Society London, Special Publications, 372. https://doi.org/10.1144/SP372.3

Herece, E. (2008). *Doğu Anadolu Fayı (DAF) Atlası*. Maden Tetkik Arama Genel Müdürlüğü Özel Yayın Serisi. No: 13, Ankara.

Herrmann, R. B. (2013). Computer programs in seismology: an evolving tool for instruction and research. *Seismological Research Letters, 84*, 1081-1088.

Higgins, M., Schoenbohm, L. M., Brocard, G., Kaymakçı, N., Gosse, J.C. & Cosca, M. A. (2015). New kinematic and geochronologic evidence for the Quaternary evolution of the Central Anatolian fault zone (CAFZ). *Tectonics, 34*, 2118-2141.

Howell, A., Jackson, J., Copley, A., McKenzie, D. & Nissen, E. (2017). Subduction and vertical coastal motions in the eastern Mediterranean. *Geophysical Journal International, 211*, 593-620.

Huang, W. (1993). Morphologic patterns of stream channels on the active Yishi Fault, southern Shandong province, eastern China: implications for repeated great earthquakes in the Holocene. *Tectonophysics, 219*, 283-304.

Huguen, C., Mascle, J., Chaumillon, E., Woodside, J. M., Benkhelil, J., Kopf, A. & Volkonskaïa, A. (2001). Deformational styles of the eastern Mediterranean Ridge and surroundings from combined swath mapping and seismic reflection profiling. *Tectonophysics, 343*, 21-47.

Jackson, J., Howell, A., Copley, A., McKenzie, D. & Nissen, E. (2019). Active tectonics of SW Turkey from the combined use of seismology, geodesy and Quaternary Geology. 72nd In H. Sözbilir, Ç. Özkaymak, B. Uzel, Ö. Sümer, M. Softa, Ç. Tepe, & S. Eski (Eds), Geological Congress of Turkey, The Proceedings and Abstracts Book, (p. 6). https://www.jmo.org.tr/resimler/ekler/174e0f6fa731893_ek.pdf

Kaya, S., Esat, K., Işık, V., Kaypak, B., Uyar, A. G. & Seyitoğlu, G. (2014). Geological and geophysical observations on the tectonic features of western part of the Afyon-Akşehir graben: a contribution to the arguments on the two-stage extension model. *Yerbilimleri, 35*, 1-16.

Kaymakçı, N., İnceöz, M., Ertepınar, P. & Koç, A. (2010). Late Cretaceous to Recent kinematics of SE Anatolia (Turkey). Geological Society London Special Publications, 340, 409–435.

Kaymakçı, N., Langereis, C., Özkaptan, M., Özacar, A.A., Gülyüz, E., Uzel, B. & Sözbilir, H. (2018). Paleomagnetic evidence for upper plate response to a STEP fault, SW Anatolia. *Earth and Planetary Science Letters, 498*, 101-115.

Keller, E. A. & Pinter, N. (2001). *Active tectonics: Earthquakes, uplift and landscape*. Prentice Hall.

Kılıç, T. & Utkucu, M. (2012). A Seismic Moment Tensor Catalogue Comprising Years 2007 and 2008 for M ≥ 4.0 Earthquakes in Turkey. *Bulletin of the Earth Sciences Application and Research Centre of Hacettepe University, 33*(3), 219-238.

Kılıç, T., Kartal, R.F., Kadirioğlu, F.T., Duman, T.Y. & Özalp, S. (2017). Türkiye ve yakın çevresi için düzenlenmiş moment tensor (1906–2012) kataloğu MW ≥ 4,0). In T.Y. Duman (Ed.), *Türkiye Sismotektonik Haritası: Maden Tetkik ve Arama Genel Müdürlüğü, Özel Yayınlar Serisi-34*, 261 s.

Koç, A. & Kaymakçı, N. (2013). Kinematics of Sürgü Fault Zone (Malatya, Turkey): A remote sensing study. *Journal of Geodynamics, 65*, 292-307.

Koçyiğit, A. & Beyhan, A. (1998). A new intracontinental transcurrent structure: The Central Anatolian Fault Zone, Turkey. *Tectonophysics, 284*, 317-336.

Kuzucuoğlu, C., Çiner, A. & Kazancı, N. (2019). The geomorphological regions of Turkey. In C. Kuzucuoğlu, A. Çiner, N. Kazancı (Eds.), *Landscapes and Landforms of Turkey* (pp. 41-178). Springer International Publishing.

Le Pichon, X. & Kreemer, C. (2010). The Miocene-to-Present kinematic evolution of the Eastern Mediterranean and Middle East and its implications for dynamics. *Annual Review of Earth and Planetary Sciences, 38*, 323-351.

Lentas, K. (2018). Towards routine determination of focal mechanisms obtained from first motion P-wave arrivals. *Geophysical Journal International, 212*, 1665–1686.

Lentas, K, Di Giacomo, D., Harris, J. & Storchak, D. A. (2019). The ISC Bulletin as a comprehensive source of earthquake source mechanisms. *Earth System Science Data, 11*, 565-578.

Mansfield, S. L. (2005). *Neogene Tectonic and Sedimentary Evolution of the Outer Cilicia Basin, Eastern Mediterranean Sea* [MSc Thesis,]. Memorial University of Newfoundland and Labrador. ISBN: 978-0-494-19380-8.

McClusky, S., Balassian, S., Barka, A., Demir, C., Ergintav, S., Georgiev, I., Gurkan, O., et al. (2000). Global Positioning System constrains on plate kinematics and dynamics in the eastern Mediterranean and Caucasus. *Journal of Geophysical Research, 105*, 5695-5719.

McKenzie, D. P. (1970). Plate tectonics of the Mediterranean Region. *Nature, 226*, 239-243.

McKenzie, D. (1972). Active tectonics of the Mediterranean Region. *Geophysical Journal of the Royal Astronomical Society, 30*, 109-185.

Melgar, D., Ganas, A., Taymaz, T., Valkaniotis, S., Crowell, B.W., Kapetanidis, V., Tsironi, V., Yolsal-Çevikbilen, S. & Öcalan, T. (2020). Rupture kinematics of 2020 January 24 Mw=6.7 Doğanyol-Sivrice, Turkey earthquake on the East Anatolian Fault Zone imaged by space geodesy. *Geophysical Journal International, 223*, 862-874.

Morelli, A. & Barrier, E. (2004). *Geodynamic map of the Mediterranean*. Commission for the Geological Map of the World, Limoges, France.

Nalbant, S. S., McCloskey, J., Steacy, S. & Barka, A. A. (2002). Stress accumulation and increased seismic risk in eastern Turkey. *Earth and Planetary Science Letters, 195*, 291-298.

Nalbant, S. S., McCloskey, J. & Steacy, S. (2005). Lessons on the calculation of static stress loading from the 2003 Bingöl, Turkey earthquake. *Earth and Planetary Science Letters, 235*, 632-640.

Okyar, M., Ergin, M. & Evans, G. (2005). Seismic stratigraphy of Late Quaternary sediments of western Mersin Bay shelf, (NE Mediterranean Sea). *Marine Geology, 220*, 113-130.

Ökeler, A. (2003). *Recent Seismicity and Stress Analysis of The Cilician Region* [Unpublished M.Sc. thesis]. Istanbul Technical University (in Turkish).

Özbakır, A. D., Şengör, A. M. C., Wortel, M. J. R. & Govers, R. (2013). The Pliny–Strabo trench region: A large shear zone resulting from slab tearing. *Earth and Planetary Science Letters, 375*, 188-195.

Özkaptan, M., Kaymakçı, N., Langereis, C. G., Gülyüz, E. & Özacar, A. A. (2018). Age and kinematics of the Burdur basin: Inferences for existence of the Fethiye Burdur Fault Zone in SW Anatolia (Turkey). *Tectonophysics, 744*, 256-274.

Papazachos, B. C. & Papaioannou, C. A. (1999). Lithospheric boundaries and plate motions in the Cyprus area. *Tectonophysics, 308*, 193-204.

Poisson, A., Wernli, R., Sağular, E. K. & Temiz, H. (2003). New data concerning the age of the Aksu Thrust in the south of the Aksu valley, Isparta Angle (SW Turkey): consequences for the Antalya Basin and the Eastern Mediterranean. *Geological Journal, 38*, 311-327.

Pondrelli, S. (2002). *European-Mediterranean Regional Centroid-Moment Tensors Catalog (RCMT) [Data set]*. Instituto Nazionale di Geofisica e Vulcanologia (INGV).

Reilinger, R. E., McClusky, S. C., Oral, M. B., King, R. W., Toksöz, M. N., Barka, A. A., et al. (1997). Global Positioning System measurements of present-day crustal movements in the Arabia-Africa-Eurasia plate collision zone. *Journal of Geophysical Research, 102*, 9983-9999.

Reilinger, R. E., McClusky, S., Vernant, P., Lawrence, S., Ergintav, S., Çakmak, R., et al. (2006). GPS constraints on continental deformation in the Africa - Arabia-Eurasia continental collision zone and implications for the dynamics of plate interactions. *Journal of Geophysical Research, 111*, Article B05411. https://doi.org/10.1029/2005JB004051

Reitman, N. G., Mueller, K. J., Tucker, G. E., Gold, R. D., Briggs, R. W. & Barnhart, K. R. (2019). Offset channels may not accurately record strike-slip fault displacement: Evidence from landscape evolution models. *Journal of Geophysical Research: Solid Earth, 124*, 13, 427-13,451.

Rojay, B., Heimann, A. & Toprak, V. (2001). Neotectonic and volcanic characteristics of the Karasu fault zone (Anatolia, Turkey): The transition zone between the Dead Sea transform and the East Anatolian fault zone. *Geodinamica Acta, 14*, 197-212.

Sage, L. & Letouzey, J. (1990). Convergence of the African and Eurasian plate in the eastern Mediterranean. In J. Letouzey (Ed.), *Petroleum and Tectonics in Mobile Belts* (pp. 49-68). 4th IFB Exploration and Production Research Conference, Bordeaux, November 14–18.

Sarıkaya, M. A., Yıldırım, C. & Çiner, A. (2015). Late Quaternary alluvial fans of Emli Valley in the Ecemiş Fault Zone, south central Turkey: Insights from cosmogenic nuclides. *Geomorphology, 228,* 512-525.

Sançar, T., Zabcı, C., Akçar, N., Karabacak, V., Yeşilyurt, S., Yazıcı, M., Akyüz, H. S., Öztüfekçi Önal, A., Ivy-Ochs, S., Christl, M. & Vockenhuber, C. (2020). Geodynamic importance of the strike-slip faults at the eastern part of the Anatolian Scholle: Inferences from the uplift and slip rate of the Malatya Fault (Malatya-Ovacık Fault Zone, eastern Turkey). *Journal of Asian Earth Sciences, 188*, Article 104091. https://doi.org/10.1016/j.jseaes.2019.104091

Savaşçın, M. Y., Francalanci, L., Innocenti, F., Manetti, P., Birsoy, R. & Dağ, N. (1995). Miocene-Pliocene potassic-ultrapotassic volcanism of the Afyon-Isparta region (central-western Anatolia, Turkey). *Petrogenesis and geodynamic implications: International Earth Sciences Colloquium on the Aegean Region (IESCA-1995), Proceedings* V-II, (pp. 487-502).

Sellier, N. C., Loncke, L., Vendeville, B. C., Mascle, J., Zitter, T., Woodside, J. & Loubrieu, B. (2013a). Post-Messinian evolution of the Florence Ridge area (Western Cyprus Arc), Part I: Morphostructural analysis. *Tectonophysics, 591*, 131-142.

Sellier, N.C., Vendeville, B. C. & Loncke, L. (2013b). Post-Messinian evolution of the Florence Rise area (Western Cyprus Arc) Part II: Experimental modeling. *Tectonophysics, 591*, 143-151.

Seyitoğlu, G., Aktuğ, B., Karadenizli, L., Kaypak, B., Şen, Ş., Kazancı, N., Işık, V., Esat, K., Parlak, O., Varol, B., Saraç, G. & İleri, İ. (2009). A Late Pliocene - Quaternary pinched crustal wedge in NW central Anatolia, Turkey: A neotectonic structure accommodating the internal deformation of the Anatolian Plate. *Geological Bulletin of Turkey, 52*(1), 121-154. https://dergipark.org.tr/tr/pub/tjb/issue/28367/301626.

Seyitoğlu, G., Ecevitoğlu, B., Kaypak, B., Esat, K., Çağlayan, A., Gündoğdu, O., Güney, Y., Işık, V., Pekkan, E., Tün, M. & Avdan, U. (2015). A missing-link in the tectonic configuration of the Almacık Block along the North Anatolian Fault Zone (NW Turkey): Active faulting in the Bolu plain based on seismic reflection studies. *Geophysical Journal International, 201*, 1814-1833.

Seyitoğlu, G., Esat, K. & Kaypak, B. (2017). The neotectonics of southeast Turkey, northern Syria and Iraq: the internal structure of the South East Anatolian Wedge and its relationship with the recent earthquakes. *Turkish Journal of Earth Sciences, 26*, 105-126.

Seyitoğlu, G., Esat, K., Kaypak, B., Toori, M. & Aktuğ, B. (2018). Internal deformation of the Turkish-Iranian Plateau in the hinterland of Bitlis-Zagros Suture Zone. In A. Farzipour Saein (ed.), *Tectonic and Structural Framework of the Zagros Fold-Thrust Belt* (pp. 161-244). Elsevier.

Seyitoğlu, G., Kaypak, B., Esat, K. & Toori, M. (2020). *The focal mechanism solution of 2020.10.25 (Mw=4.1) Sancaklı-Bingöl Earthquake and an evaluation of the seismicity along the Southeast Anatolian Zagros Fault Zone*. Researchgate Technical Report. http://doi.org/10.13140/RG.2.2.23793.10083

Seyitoğlu, G., Esat, K., Kaypak, B. & Çıvgın, B. (2022) *Seismotectonics of the southern branch of North Anatolian Fault Zone along Bolu – Bursa – İzmir – Değirmenlik (Milos) island in the Aegean Sea*. In review.

Seymen, İ. & Aydın, A. (1972). The Bingöl earthquake fault and its relation to the North Anatolian fault zone. *Bulletin of the Mineral Research and Exploration, 79*, 8-12.

Shaw, B. & Jackson, J. (2010). Earthquake mechanisms and active tectonics of the Hellenic subduction zone. *Geophysical Journal International, 181*, 966-984.

Symeou, V., Homberg, C., Nader, F.H., Darnault, R., Lecomte, J-C. & Papadimitriou, N. (2018). Longitudinal and temporal evolution of the tectonic style along Cyprus Arc System, assessed through 2-D reflection seismic interpretation. Tectonics, 37, 30-47.

Şaroğlu, F., Emre, Ö. & Kuşçu, İ. (1992). The East Anatolian Fault Zone of Turkey. In R.C. Bucknam, & P.L. Hancock (Eds.), *Major active faults of the world, results of IGCP project 206*. Annales Tectonicae, suppl vol IV, 99-125.

Şengör, A. M. C. (1980). *Türkiye'nin Neotektoniğinin Esasları [Fundamentals of the neotectonics of Turkey]*. Publication of Geological Society of Turkey, pp 1-40.

Şengör, A. M. C. (2017). Diversion of river courses across major strike-slip faults and keirogens. In İ. Çemen & Y. Yılmaz (Eds.), *Active Global Seismology: Neotectonics and Earthquake Potential of the Eastern Mediterranean Region* (pp. 93-101). Geophysical Monograph 225.

Şengör, A. M. C. & Barka, A. (1992). Evolution of escape-related strike-slip systems: implications for disruption of collisional orogens. *In 29th International Geological Congress* (p.:323). Kyoto, Japan, Abstracts, vol. 1, p. 232.

Şengör, A. M. C., Görür, N. & Şaroğlu, F. (1985). Strike-slip deformation basin formation and sedimentation: Strike-slip faulting and related basin formation in zones of tectonic escape: Turkey as a case study. In K.T. Biddle & N. Christie-Blick (Eds.), *Strike-slip faulting and basin formation* (pp.227-264). Society of Economic Paleontologist and Minerologists Special Publications 37.

Şengör, A. M. C., Tüysüz, O., İmren, C., Sakınç, M., Eyidoğan, H., Görür, N., Le Pichon, X. & Rangin, C. (2004). The North Anatolian Fault: A new look. *Annual Review of Earth Planetary Sciences, 33,* 1-75.

Şengör, A. M. C., Zabcı, C. & Natal'in, B. A. (2019). Chapter 9 - Continental Transform Faults: Congruence and Incongruence with Normal Plate Kinematics? In J. C. Duarte (Ed.), *Transform Plate Boundaries and Fracture Zones* (pp. 169-247). Elsevier. https://doi.org/10.1016/B978-0-12-812064-4.00009-8

Umhoefer, P. J., Thomson, S. N., Lefebvre, C., Cosca, M. A., Teyssier, C. & Whitney, D. L. (2020). Cenozoic tectonic evolution of the Ecemiş Fault Zone and adjacent basins, central Anatolia, Turkey, during the transition from Arabia-Eurasia collision to escape tectonics. *Geosphere, 16*, 1358-1384.

Walsh-Kennedy, S., Aksu, A. E., Hall, J., Hiscott, R. N., Yaltırak, C. & Çifçi, G. (2014). Source to sink: The development of the latest Messinian to Pliocene–Quaternary Cilicia and Adana Basins and their linkages with the onland Mut Basin, eastern Mediterranean. *Tectonophysics, 622*, 1-21.

Westaway, R. & Arger, J. (2001). Kinematics of the Malatya-Ovacık Fault. *Geodinamica Acta, 14,* 103-131.

Woodside, J. M. (1977). Tectonic elements and crust of Eastern Mediterranean Sea. *Marine Geophysical Research, 3*, 317-354.

Woodside, J. M., Mascle, J., Huguen, C. & Volkonskaia, A. (2000). The Rhodes Basin, a post-Miocene tectonic trough. *Marine Geology, 165*, 1-12.

Woodside, J. M., Mascle, J., Zitter, T. A. C., Limonov, A. F., Ergün, M. & Volkonskaia, A. (2002). The Florence Rise, the western bend of the Cyprus Arc. *Marine Geology, 185*, 177-194.

Yazıcı, M., Zabcı, C., Sançar, T. & Natalin, B. A. (2018). The role of intraplate strike-slip faults in shaping the surrounding morphology: The Ovacık Fault (eastern Turkey) as a case study. *Geomorphology, 312*, 129-145.

Yetiş, C. (1978). Geology of the Çamardı (Niğde) region and the characteristics of the Ecemiş Fault Zone between Madenboğaz and Kamışlı. *Istanbul University, Faculty of Science Bulletin, Serie B, 43*, 41-61.

Yıldırım, C., Sarıkaya, M. A. & Çiner, A. (2016). Late Pleistocene intraplate extension of the Central Anatolian Plateau, Turkey: Inferences from cosmogenic exposure dating of alluvial fan, landslide, and moraine surfaces along the Ecemiş Fault Zone. *Tectonics, 35*, 1446-1464.

Yolsal-Çevikbilen, S. & Taymaz, T. (2012). Earthquake source parameters along the Hellenic subduction zone and numerical simulations of historical tsunamis in the Eastern Mediterranean. *Tectonophysics, 536-537*, 61-100.

Zhang, K., Liu, K. & Yang, J. (2004). Asymmetrical valleys created by the geomorphic response of rivers to strike-slip fault. *Quaternary Research, 62*, 301-315.

Zitter, T. A. C., Woodside, J. M. & Mascle, J. (2003). The Anaximander Mountains: a clue to the tectonics of southwest Anatolia. *Geological Journal, 38*, 375-394.

Zoback, M. L. (1992). First- and second-order patterns of stress in the lithosphere: The World Stress Map project. *Journal of Geophysical Research, 97*, 11703-11728.